

# Cranial osteology and ontogeny of *Saurolophus angustirostris* from the Late Cretaceous of Mongolia with comments on *Saurolophus osborni* from Canada

PHIL R. BELL



Bell, P.R. 2011. Cranial osteology and ontogeny of *Saurolophus angustirostris* from the Late Cretaceous of Mongolia with comments on *Saurolophus osborni* from Canada. *Acta Palaeontologica Polonica* 56 (4): 703–722.

Reanalysis of the skull of the crested Asian hadrosaurine *Saurolophus angustirostris* confirms its status as a distinct species from its North American relative, *Saurolophus osborni*. In addition to its greater absolute size, *S. angustirostris* is differentiated from *Saurolophus osborni* by an upturned premaxillary body, a more strongly reflected oral margin of the premaxilla, the absence of an anterior notch in the prenasal fossa, a sigmoidal contour of the ventral half of the anterior process of the jugal, a shallow quadratojugal notch on the quadrate, and by a strongly bowed quadrate in lateral view. Phylogenetic analysis corroborates a sister taxon relationship between *S. angustirostris* and *S. osborni*. *Saurolophus* itself is characterised by a solid, rod-like crest composed of the nasals, frontals, and prefrontals; secondary elongation of the frontal and prefrontal resulting in the backwards extension of the frontal platform; a frontal platform that extends dorsal to the anterior portion of the supratemporal fenestra; a parietal that is excluded by the squamosals from the posterodorsal margin of the occiput; and the presence of two supraorbital elements. Although the palaeobiogeographic history of *Saurolophus* remains unresolved, at least two possible dispersal events took place across Beringia during the late Campanian leading to the evolution of the clade composed of *Kerberosaurus*, *Prosaurolophus*, and *Saurolophus*.

Key words: Dinosauria, Ornithischia, Hadrosauridae, Hadrosaurinae, *Saurolophus*, taxonomy, Cretaceous, Mongolia.

Phil R. Bell [pbell@ualberta.ca], Department of Biological Sciences, University of Alberta, Edmonton, T6G 2E9, Canada.

Received 26 June 2010, accepted 25 December 2010, available online 4 January 2011.

## Introduction

The Upper Cretaceous beds of southern Mongolia are famous for their well-preserved and diverse dinosaur fauna. The ?late Campanian/early Maastrichtian Nemegt Formation alone has yielded tyrannosaurids, ornithomimids, oviraptorids, therizinosaurs, alvarezsaurids, troodontids, dromaeosaurids, avimimids, elmsaurids, ankylosaurids, hadrosaurids, and pachycephalosaurids (Weishampel et al. 2004). This diversity is palaeobiogeographically important as it is replicated in coeval beds from western North America, at least at the family level (Jerzykiewicz and Russell 1991). The only genus to occur in both regions is the hadrosaurid *Saurolophus*, represented by *Saurolophus angustirostris* from Mongolia and *Saurolophus osborni* from western Canada.

*Saurolophus osborni* was erected based on a virtually complete skull and skeleton from the early Maastrichtian upper Horseshoe Canyon Formation in southern Alberta, Canada (Brown 1912). The genus is notable for its solid rod-like cranial crest, which is comprised of the nasals, prefrontals, and frontals (Brown 1912; Bell 2011).

Between 1946 and 1949, the Soviet Palaeontological Expeditions to central Mongolia collected multiple skeletons of a new hadrosaurid from the localities of Nemegt and Altan Uul. Rozhdestvensky (1952) named the new animal *Saurolophus angustirostris*, stressing the gross similarity between

immature specimens of that species to adults of its North American relative (Rozhdestvensky 1952, 1957, 1965). In the Nemegt Formation, *S. angustirostris* comprises approximately 20% of all vertebrate fossils (Currie 2009) found, whereas only three unequivocal specimens of *S. osborni* have so far been recovered from the Horseshoe Canyon Formation. Two incomplete specimens from the Moreno Formation, California, were designated as cf. *Saurolophus* by Morris (1973); however, the best-preserved specimen has recently been reassigned to Hadrosaurinae indet. (Bell and Evans 2010). A partial “booted” ischium from the Amur region of far Eastern Russia was designated the type of *Saurolophus kryshchovici* by Riabinin (1930) based on comparison with the equally dubious plesiotype (AMNH 5225) of *S. osborni*. The plesiotype, an isolated but complete ischium from the same area as the holotype, was provisionally re-identified by Russell and Chamney (1967) as *Hypacrosaurus*; and *S. kryshchovici* is unanimously regarded as a nomen dubium (Young 1958; Maryńska and Osmólska 1981; Weishampel and Horner 1990; Norman and Sues 2000; Horner et al. 2004).

The close similarity between the Mongolian and the Canadian species of *Saurolophus* has led some authors to question the validity of *S. angustirostris*. In a supplementary descrip-

Table 1. Select cranial measurements (mm) for *Saurolophus angustirostris* Rozhdestvensky, 1952 and *Saurolophus osborni* Brown, 1912. Abbreviations: b, Brown 1912; i, image J; L, left; R, right; #, incomplete; \*, reconstructed; ~, approximate; >, more than; ^, based on 6 teeth per 5 cm, tooth row length 390 mm.

|  | <i>Saurolophus angustirostris</i> |             |             |             |             |             |             |             |                |                | <i>Saurolophus osborni</i> |                      |          |
|--|-----------------------------------|-------------|-------------|-------------|-------------|-------------|-------------|-------------|----------------|----------------|----------------------------|----------------------|----------|
|  | PIN 551/356 (holotype)            | PIN 551/359 | PIN 551/357 | PIN 551/358 | PIN 551/407 | UALVP 49067 | MPC 100/706 | MPC 100/764 | ZPAL MgD-1/159 | ZPAL MgD-1/162 | AMNH 5220 (holotype)       | AMNH 5221 (paratype) | CMN 8796 |
| Premaxila to quadrate: length                  | 950                               | 575         | 1220        | 1025        |             | 580         | 1200        |             | 437            |                | 1000b                      |                      | 945      |
| Premaxila to tip of crest: length              | 1350                              | 670         |             |             |             | 740         | 1770        |             | 485            |                | 1170b                      |                      | 950#     |
| Premaxilla: length                             | 760                               | 380         | ~900        | ~1210       |             | 375         | 890#        |             | 255            |                | 780i                       | 660                  | 680      |
| Premaxilla: length of dorsal ramus from naris  | 340                               | 145         |             | 370         |             | 165         | 510         | 380         | 50             |                | 324i                       | 230#L, 260#R         | >285     |
| Premaxilla: length of ventral ramus from naris | 495                               | 260         | ~650        | ~890        |             | 240         | 700#        | 650         | 149            |                | 548i                       | 450                  | 430      |
| Quadrate: height                               | 395                               | 260         | 460         | 545         |             | 240         | 485         |             | 215            | 395            | 365                        | 375                  | 385*     |
| Crest: length                                  | 405                               | 200         |             |             |             |             | 570         |             | 150            |                | 307i                       |                      | 115#     |
| Naris: length                                  | 230                               | 90          | 165         | 195         |             | 160         | 370         | 215         | 55             |                | 352i                       |                      |          |
| Mandible: length                               | 955                               | 565         |             | 1260        |             | 600         | 1120        |             | 415            |                | 951i                       |                      | 910      |
| Dentary: length                                | 770                               | 450         | 1025        | 1030        | 940         | 440         | 940         |             | 335            |                |                            | 425#L, 370#R         | 730      |
| Dentary: length of edentulous portion          | 330                               | 170         | 450         | 450         | 380         | 160         | 380         |             | 130            |                |                            |                      | 290      |
| Dentary: tooth count                           |                                   |             |             |             | 50          |             | 46          | >29         | >26            |                |                            | 43#L, 43#R           |          |
| Maxilla: ventral length                        |                                   | 290         | 580         |             |             |             | 590         |             |                | 390            |                            | 450                  | 450      |
| Maxilla: tooth count                           |                                   | >35         | >50         |             |             |             |             | >44         | >27            |                |                            | 46^                  |          |
| Nasal: length                                  | ~170                              | 580         |             | 1020#       |             | 625         | 1495        |             | 378            |                | 994i#                      |                      | 780*     |
| Frontal: length posterodorsal process          | 105                               |             |             |             |             |             | 220         |             | ~10            |                |                            |                      |          |
| Jugal: length                                  | 345                               | 230         |             | 410         |             | 185         | 400         | 390         | 183            | 307            | 340                        | 315                  | 340      |

tion of that species, Maryńska and Osmólska (1984) listed eight cranial characters that apparently distinguished *Saurolophus angustirostris* from other hadrosaurids; however, Norman and Sues (2000) argued that the diagnostic characters listed by Maryńska and Osmólska (1984) for *S. angustirostris* may fall into the realm of individual variation. Horner (1992) later attempted to distinguish the two species by the presence of a “frontal buttress” (posterodorsal process sensu Bell 2011) in only *S. angustirostris*. This feature has since been identified as a synapomorphy of the genus (Bell 2011).

*Saurolophus angustirostris* is represented by multiple well-preserved skulls, the largest of which (PIN 551/357) is approximately 300% longer than the smallest (ZPAL MgD-1/159) specimen (Table 1). These specimens provide the opportunity to separate phylogenetically important characters from individual and ontogenetic variation. The purpose of this study is to redescribe the skull of *S. angustirostris* with a focus on ontogenetic and individual variation (particularly

the braincase and cranial crest) and to provide an updated diagnosis of the genus. Where possible, bones of *S. angustirostris* are compared with the corresponding element in *S. osborni* described in detail by Bell (2011) in order to reassess the interrelationships of these two species.

*Institutional abbreviations.*—AMNH, American Museum of Natural History, New York, USA; CMN, Canadian Museum of Nature, Ottawa, Ontario, Canada; KID, Hwaseong Paleontological Laboratory, Hwaseong City, South Korea; LACM/CIT, Natural History Museum of Los Angeles County (specimen formerly housed at the California Institute of Technology), Los Angeles, California, USA; MOR, Museum of the Rockies, Bozeman, Montana, USA; MPC, Mongolian Palaeontological Centre, Ulaan Baatar, Mongolia; PIN, Palaeontologičeski Institut, Akademii Nauk, Moscow, Russia; UALVP, University of Alberta Laboratory for Vertebrate Paleontology, Edmonton, Alberta, Canada; ZPAL, Institute of Palaeobiology of the Polish Academy of Sciences, Warsaw, Poland.

## Material and methods

Descriptions of *Saurolophus angustirostris* are based on an ontogenetic series represented by KID 476 (partial adult skull), ZPAL MgD-1/159 (juvenile skull and partial skeleton), ZPAL MgD-1/162 (partial subadult skull), ZPAL MgD-1/173 (partial subadult skull), MPC 100/706 (adult skull and skeleton), MPC 100/764 (adult skull), PIN 551/8 (holotype; subadult skull and skeleton), PIN 551/357 (partial adult skull), PIN 551/358 (adult skull), PIN 551/359 (juvenile skull), PIN 551/407 (adult mandible), UALVP49067 (subadult skull). All specimens come from the late ?Campanian–Maastrichtian Nemegt Formation from the areas of Nemegt and Altan Uul, Mongolia except UALVP49067 and MPC 100/764, which are of unknown provenance.

All definitive specimens of *S. osborni* were included in the comparisons: AMNH 5220 (holotype; adult skull and skeleton), AMNH 5221 (paratype; adult skull and partial postcrania), CMN 8796 (adult skull).

Age class designations follow Evans' (2010) adaptation of Horner et al. (2000) where "juvenile" corresponds to a skull length of less than 50% of the maximum observed skull length. "Subadults" are defined as individuals with a skull length of 50–85% and "adults" are greater than 85% of the maximum observed skull length.

## Systematic palaeontology

Dinosauria Owen, 1842

Ornithischia Seeley, 1887

Ornithopoda Marsh, 1881

Hadrosauridae Cope, 1869

Hadrosaurinae Lambe, 1918

Genus *Saurolophus* Brown, 1912

*Emended diagnosis*.—Large hadrosaurine hadrosaurid (up to 12 m long) with the following apomorphies: solid, caudo-dorsally-directed cranial crest composed of the nasals, prefrontals, and frontals that extends posterior to the squamosals in adults; posterodorsal process of prefrontal and frontal united to form dorsal promontorium that buttresses the underside of the nasal crest; frontals tripartite. Differs from other hadrosaurines with the combination of additional characteristics: frontals excluded from the orbital rim by the post-orbital-prefrontal complex; two supraorbital elements; parietal excluded by the squamosals from posterodorsal margin of occiput.

*Saurolophus angustirostris* Rozhdestvensky, 1952

*Holotype*: PIN 551/8.

*Type locality*: Nemegt, Mongolia.

*Type horizon*: Nemegt Formation (?upper Campanian/lower Maastrichtian), Upper Cretaceous.

*Emended diagnosis*.—Differs from *S. osborni* in having a

skull that is at least 20% longer among the largest adults; premaxilla with strongly reflected oral margin and upturned premaxillary body in lateral aspect; broadly arcing anterior margin of the preauricular fossa; an elongate, anteriorly directed spur on the anterior process of the jugal that separates the lacrimal and maxilla, more so than in *S. osborni*; shallow quadratojugal notch on the quadrate; and more strongly bowed quadrate in lateral view.

## Comparative description of the skull of *S. angustirostris*

### General skull

The skull is typically hadrosaurine in general morphology (see descriptions) and forms a right triangle in lateral view at its ventral and posterior edges (Fig. 1). The largest specimens are significantly longer than the largest skulls of *S. osborni* ( $t$ -test = 3.18, degrees of freedom = 3,  $\alpha$  = 0.05). The most conspicuous feature of the skull is the solid, rod-like crest that extends posterodorsally from the skull roof and which projects beyond the squamosals in the largest specimens. In juveniles, the orbit is shaped like an inverted pear, but in adults it is posterodorsally reclined from the vertical and dorsoventrally elongate. The infratemporal fenestra forms a posterodorsally elongate ellipse and the supratemporal fenestra is elliptical.

**Premaxilla**.—The paired premaxillae form the anterior oral margin and contribute at least 50% of the length of the skull (measured from the anterior tip of the premaxilla to the posterior tip of the nasal crest). In lateral view, the body of the premaxilla is strongly upturned and the lateral margins are reflected, more so than *Gryposaurus* or *Prosaurolophus*, but not as exaggerated as *Edmontosaurus regalis* (CMN 2288). In *S. osborni*, the dorsal margin of the premaxilla is straight in lateral view and the oral margin is only weakly reflected, similar to *Prosaurolophus*. The lateral premaxillary margins of *S. angustirostris* are perforated by numerous small foramina. Along the midline, the premaxillae meet to form a sharp sagittal keel that extends the length of the body of the premaxilla. The premaxillae fuse anteriorly only in adults. In articulated specimens viewed dorsally, the posterodorsal process of *S. angustirostris* is visible until it reaches the posterior margin of the external naris and attenuates posteriorly under the nasals. It extends posteriorly beyond this point, although its posterior terminus is obscured by the nasals. The posterodorsal process is triangular in cross-section for its entire length. The posterolateral process is plate-like. It extends posteriorly over the lacrimal without meeting the prefrontal, typical of most hadrosaurines except *Maiasaura* (Horner 1983) and *Brachylophosaurus* (CMN 8893), where it is notably shorter. The entire posterolateral process maintains a consistent width where it forms the ventral margin of the external narial foramen. It tapers gradually posterior to that fo-

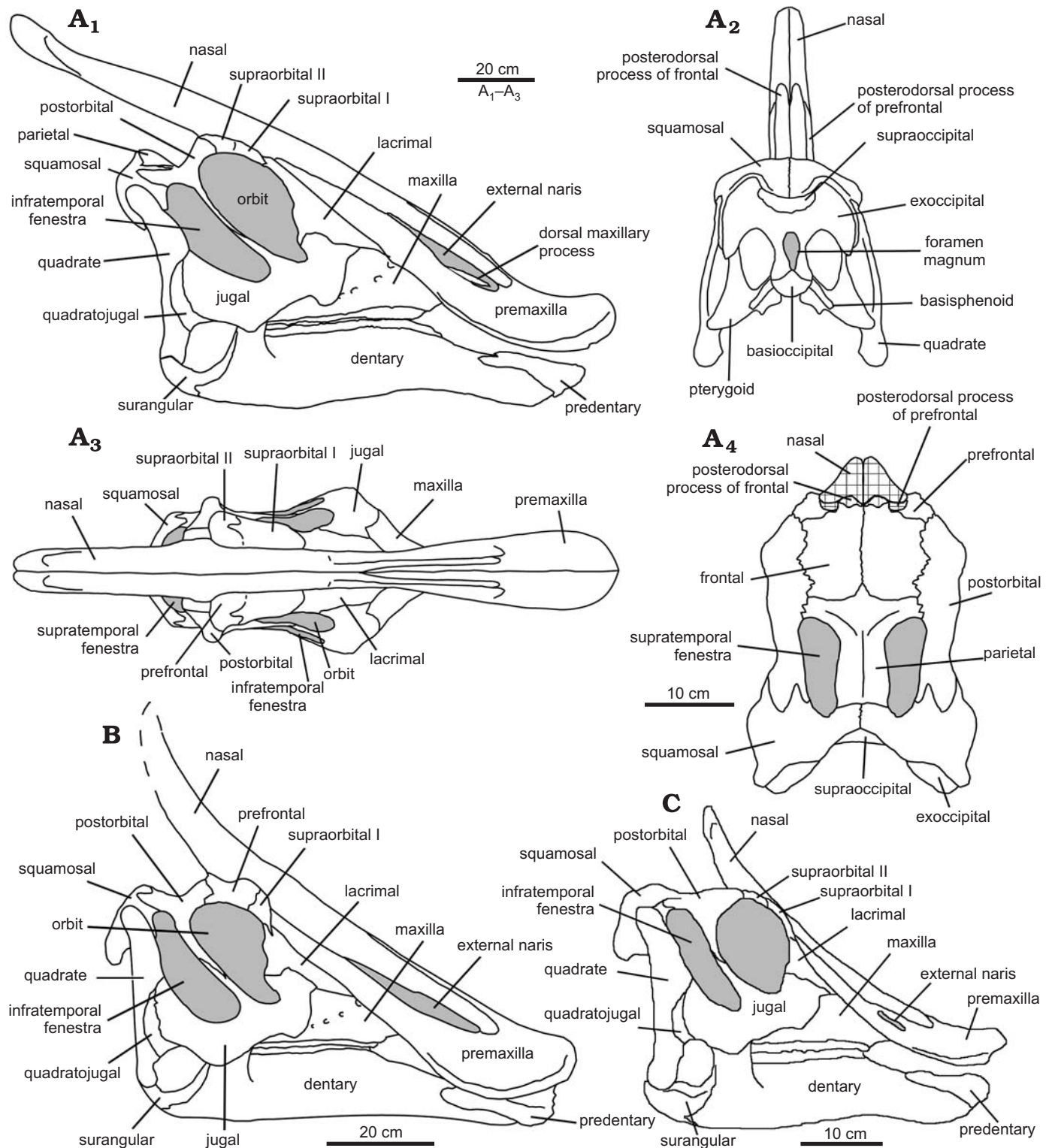


Fig. 1. Adult *Saurolophus* skulls compared. **A.** *Saurolophus angustirostris* Rozhdestvensky, 1952, based on MPC 100/706, late Campanian–?Maastrichtian Nemegt Formation, Mongolia; in lateral ( $A_1$ ), posterior ( $A_2$ ), and dorsal ( $A_3$ ) view. Skull roof with crest removed as denoted by cross-hatching ( $A_4$ ). **B.** Skull of *Saurolophus osborni* Brown, 1912, AMNH 5220, Maastrichtian Horseshoe Canyon Formation, Alberta, Canada; in lateral view. Dashed lines imply inferred margins.

ramen. The position of the anterior border of the prenasal fossa is ontogenetically variable. It forms a wide arc that is confluent with the anterior border of the external narial fora-

men in adults (Fig. 2) but which is situated well forward of this foramen in juveniles. It is unclear if this character is ontogenetically variable in *S. osborni*, as only adult speci-

mens are known. In *Saurolophus osborni* (AMNH 5221), the prenarial fossa extends anteriorly from the naris forming a long, narrow groove on the lateral surface of the premaxillary body. This extension is distinct from the broad arc seen in *S. angustirostris*.

**Maxilla.**—The outline of the maxilla forms a roughly symmetrical isosceles triangle in lateral view as in other hadrosaurines (Horner et al. 2004). The ventral margin is slightly concave ventrally and has more than 27 alveoli in ZPAL MgD-1/159 but more than 45 in the largest individuals (Table 1). Up to four (possibly five) teeth are present in each alveolus. The anterodorsal process is separated ventrally from the anterior tip of the maxilla by a sulcus. It is medio-laterally compressed and, in both juvenile and adult specimens, is visible through the external narial foramen where it almost reaches the anterior limit of that fenestra (Fig. 2). Equally long anterodorsal processes have been reported in *Maiasaura* (Horner 1983), *Brachylophosaurus* (Prieto-Marquez 2005; Cuthbertson and Holmes 2010), and *Gryposaurus monumentensis* (see Gates and Sampson 2007). This process is either broken or is unprepared in specimens of *S. osborni* and therefore cannot be compared. The anterodorsal process abuts the underside of the premaxilla on its dorso-medially-inclined lateral surface. Dorsally, there is a prominent groove that migrates medially onto the distal end of the anterodorsal process that contacts the vomer (Horner 1992). Up to seven foramina, which decrease in diameter posteriorly, perforate the lateral surface of the maxilla. The most anterior foramen forms a notch in the anterodorsal edge of the maxilla. In well-preserved specimens, the notch is partly covered by a tabular process on the lateral margin of the premaxilla. The contact with the premaxilla obscures a probable contact with the nasal in this region. The dorsal process lies at about the midlength of the maxilla. It contacts the lacrimal anteriorly and the jugal dorsally and laterally. The lateral contact for the jugal is furrowed ventrally and smooth dorsally. The posterior end of the maxilla cannot be fully viewed in any specimen, but is low and subrectangular in lateral view, as in *Prosaurolophus* and *Edmontosaurus* (Lambe 1920; Horner 1992).

**Nasal.**—The nasals are the longest bones in the skull and are in contact for most of their length, meeting along their extensive, flat medial surfaces. The nasals remain unfused even in large specimens. Anteriorly, the nasals are mediolaterally flattened and separated by the posterodorsal processes of the premaxillae. Each nasal forms the entire dorsal margin of the external narial foramen and extends beyond the anterior limit of that foramen. This condition otherwise occurs only in *Prosaurolophus* (ROM 1928, CMN 2277), *Edmontosaurus* (CMN 8509, CMN 2288), and *S. osborni*. In all other hadrosaurines, the nasal does not extend the length of the naris and/or contributes along with the premaxilla to the dorsal margin of the narial opening. Posterior to the naris, the nasal is taller and wider, becoming triangular in cross-section. At the point where the nasal overlies the frontal and prefrontal, it

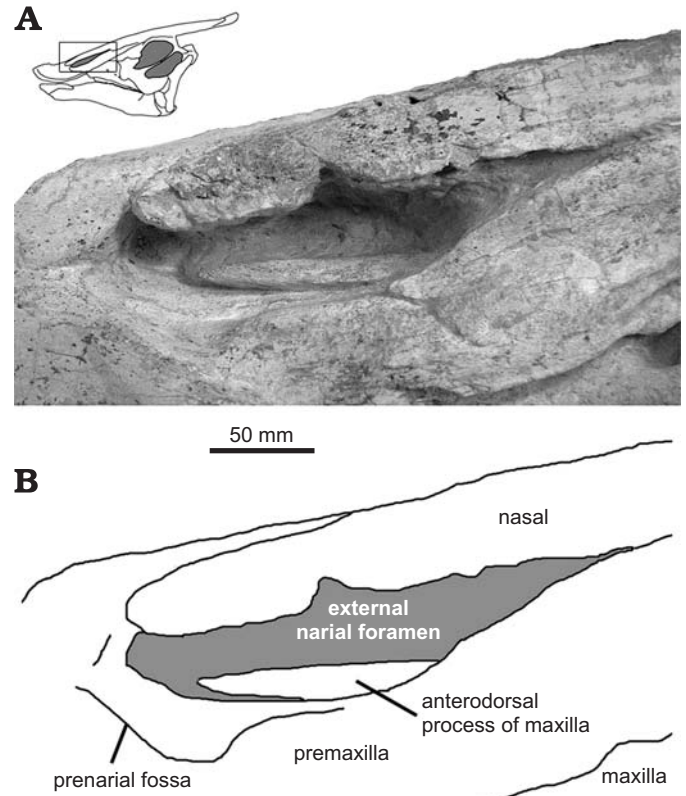
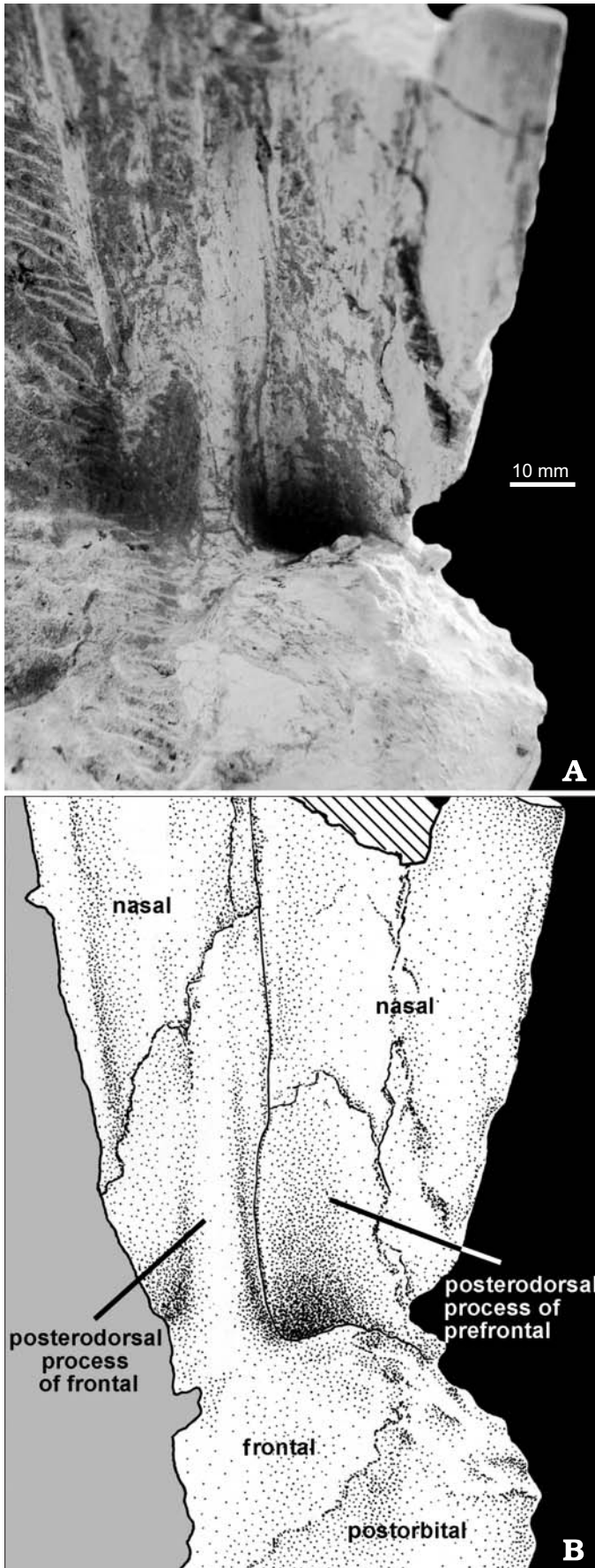


Fig. 2. Details of the left narial region in an adult *Saurolophus angustirostris* Rozhdestvensky, 1952, MPC 100/764; late Campanian–?Maastrichtian Nemegt Formation, Mongolia, as demarcated by the boxed area on inset. Photograph (A) and explanatory drawing (B). Note the elongate anterodorsal process of the maxilla. Grey indicates matrix.

extends posterodorsally to participate in the solid crest. The crest is roughly triangular in cross-section and extends beyond the posterior margin of the skull in the largest specimens. The proximal half of the crest is braced ventromedially by thin processes from the frontals and ventrolaterally by the prefrontals (Fig. 3). There are numerous longitudinal grooves on the underside of the crest that likely served to strengthen this contact. In small and mid-sized specimens with short crests, the nasals are relatively straight in lateral view and the crest is consequently steeply elevated. In larger individuals, the crest extends beyond the posterior margin of the occiput and is less steeply elevated, which gives the nasal a “bent” appearance in lateral view (Fig. 1A<sub>1</sub>). Although an ontogenetic series is unknown for *S. osborni*, the nasals are straight and approximate the immature condition of *S. angustirostris* (Rozhdestvensky 1952, 1957); the crest is steeply angled and does not extend past the posterior margin of the skull (Fig. 1B). The distal end of the crest is unknown in *S. osborni*. In *S. angustirostris* the nasal terminates in a thickened bony “swelling”, which has been referred to as the posterior border of the circumnarial fossa (Maryńska and Osmólska 1979; Horner 1992; Godefroit et al. 2008). The dorsal surface of this distal swelling is marked by several posterolaterally-directed furrows. The anterior edge of the swelling is excavated, forming a cavity. A subtle, postero-



laterally-oriented ridge on the anterior (dorsal) surface of the nasal extends to meet the lateral edge of the distal swelling. A second longitudinal ridge is present anteriorly near the anterior base of the crest. These ridges are synonymous with the longitudinal bony septum described by Maryńska and Osmólska (1979).

**Jugal.**—The jugal is W-shaped in lateral aspect and forms the ventral borders of both the orbit and infratemporal fenestra. The anterior process is asymmetrical in small and medium sized animals, becoming more (but not entirely) symmetrical in the largest skulls (PIN 551-358, MPC 100/706). Medially, this process broadly overlies the maxilla and the ventral edge of the lacrimal. The jugal does not reach the premaxilla as it does in *Edmontosaurus* (CMN 2288, CMN 8509). In lateral view, the anterior process tapers to an elongate spur that separates the maxilla and lacrimal for some distance (Figs. 1A, 4). This spur gives the ventral contour of the anterior process a sigmoidal outline similar to *Edmontosaurus*. This spur is consistently short in *Saurolophus osborni* and the ventral outline of the anterior process is subsequently more convex (Fig. 4; Gates and Sampson 2007). The straight postorbital process is angled posteriorly in *Saurolophus* and *Prosaurolophus*. In other hadrosaurines, this process is nearly vertical except in *Edmontosaurus* and *Brachylophosaurus* where it is strongly retroverted (Gates and Sampson 2007; Cuthbertson and Holmes 2010). The distal end of the postorbital process is antero-posteriorly flattened for contact with the posterior edge of the reciprocal process of the postorbital. The posterior process is tabular and the jugal flange only moderately developed as in *S. osborni*, *Prosaurolophus* (CMN 2277, ROM 1928), and *Edmontosaurus* (CMN 2288, CMN 8509). The posterior process overlies much of the quadratojugal, excluding it from the margin of the infratemporal fenestra.

**Quadratojugal.**—The quadratojugal is subtriangular and incompletely separates the quadrate and the jugal. The ventral margin is concave and forms an acute angle with the posterior margin of the quadratojugal. This angle is about  $77^\circ$  in *S. osborni* (AMNH 5221) and *S. angustirostris* (MPC 100/706); wider than in *Brachylophosaurus* ( $66^\circ$ , MOR 1071-7-15-98-218A). In *Edmontosaurus* (Lambe 1920), the posterior margin of the quadratojugal is so convex as to make this measurement equivocal. In contrast, the posterior margin in *Saurolophus* is relatively weakly convex as in *Prosaurolophus* (ROM 787, ROM 1928). Posteromedially, the quadratojugal forms a lap joint with the corresponding facet on the quadrate. The quadratojugal is mediolaterally widest posteriorly and tapers anteriorly where it is covered laterally by the posterior process of the jugal. The quadratojugal of *S. osborni* is virtually identical to that of *S. angustirostris*.

Fig. 3. Posterior view of the proximal crest in hadrosaurid dinosaur *Saurolophus angustirostris* Rozhdestvensky, 1952, MPC 100/764, late Campanian–?Maastrichtian Nemegt Formation, Mongolia; right side. Shading indicates matrix. Cross-hatching indicates broken cross-section of nasal. Dorsal is up. Photograph (A) and explanatory drawing (B).

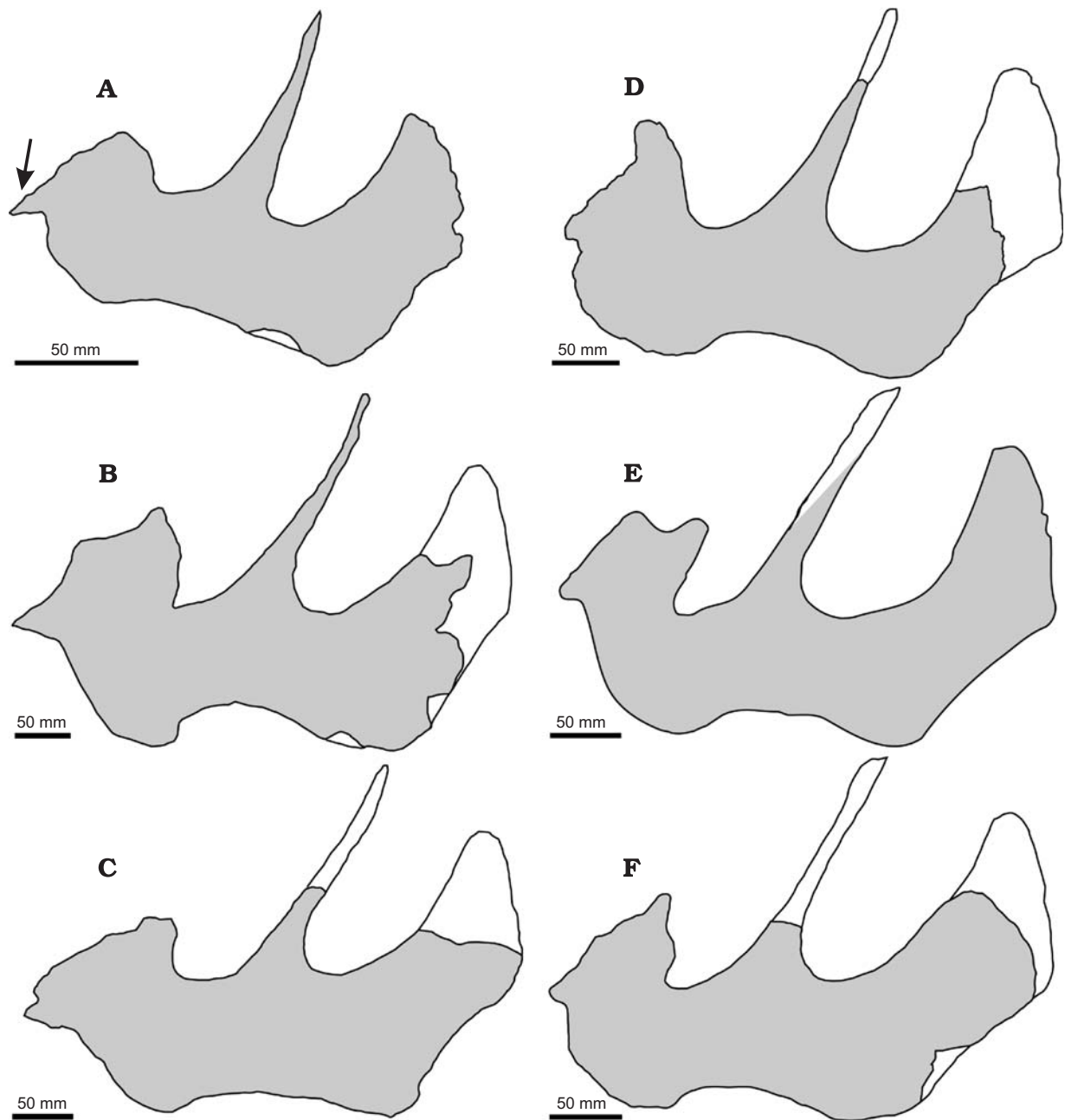


Fig. 4. Jugals of *Saurolophus*. **A–C.** *Saurolophus angustirostris* Rozhdestvensky, 1952, late Campanian–?Maastrichtian Nemegt Formation, Mongolia. **D–F.** *Saurolophus osborni* Brown, 1912, Maastrichtian Horseshoe Canyon Formation, Alberta, Canada. **A.** ZPAL MgD-1/159 juvenile. **B.** MPC 100/706 adult. **C.** MPC 100/764 adult. **D.** AMNH 5221 adult, reversed. **E.** AMNH 5220 adult, reversed. **F.** CMN 8796 adult, reversed. Note the anteriorly-directed spur on the anterior process in *S. angustirostris* (arrow) is prominent in even the juvenile. This process is reduced in *S. osborni*. White represents reconstructed areas. Anterior is left.

**Quadrate.**—The quadrate is rod-like and forms the posterior margin of the skull in lateral view. In all specimens of *S. angustirostris*, it is more strongly bowed in comparison to *Saurolophus osborni*, *Edmontosaurus* (CMN 8509, Lambe 1920), *Prosaurolophus* (Horner 1992), or *Gryposaurus* (Gates and Sampson 2007). In dorsal aspect, the squamosal articular facet of the quadrate is subtriangular in outline. The quadratojugal notch occupies approximately the middle third of the quadrate. It forms a shallow, symmetrical “C” along its anterior margin that differs from the asymmet-

rical notch in *Gryposaurus* (Gates and Sampson 2007) and the deeply incised notch in *S. osborni* and *Edmontosaurus* (Fig. 5; Lambe 1920). Ventral to the quadratojugal notch, the quadrate is expanded mediolaterally to form a mandibular condyle that is roughly trapezoidal in dorsal section; the medial condyle is reduced and indistinct, typical of hadrosaurids (Horner et al. 2004). The pterygoid process extends antero-medially from the posteromedial surface of the quadrate. This process is slender, roughly triangular in lateral view, and extends nearly the entire height of the quadrate. The me-

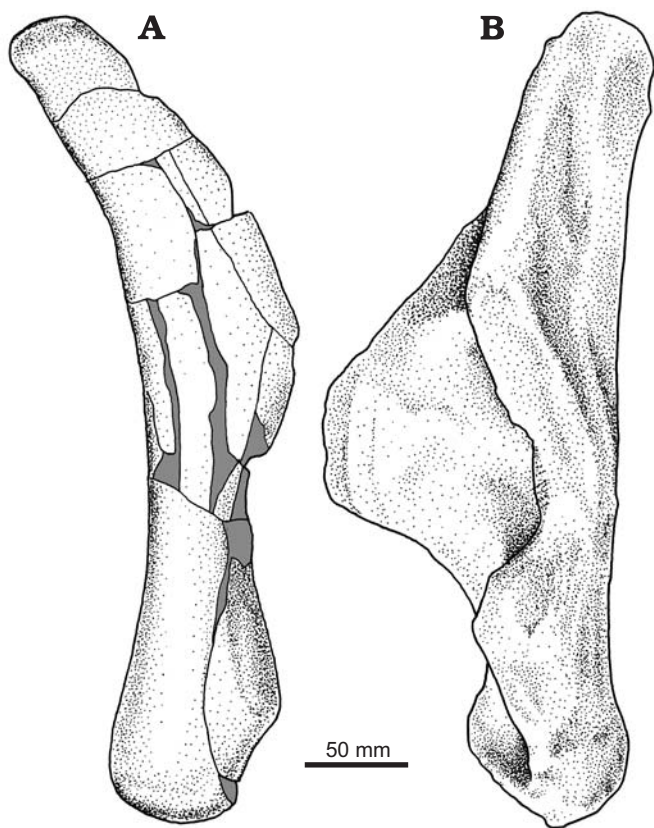


Fig. 5. Comparison of quadrates of *Saurolophus* in lateral view. **A.** Right quadrate of *Saurolophus angustirostris* Rozhdestvensky, 1952, ZPAL MgD-1/163, late Campanian–?Maastrichtian Nemegt Formation, Mongolia. **B.** Left quadrate of *Saurolophus osborni* Brown, 1912, AMNH 5220, Maastrichtian Horseshoe Canyon Formation, Alberta, Canada; modified from Bell (2011). Grey regions indicate broken surfaces. Dorsal is up.

dial surface of the pterygoid process is covered by the quadrate processes of the pterygoid.

**Squamosal.**—The squamosals forms the posterior border of the skull roof, including the posterior margin of the supratemporal fenestrae. There are four processes that originate posterolaterally. Extending medially and dorsally, the parietal process contacts its counterpart along the median sagittal plane to exclude the parietal from the posterior margin of the skull as in *Maiasaura* and Lambeosaurinae (Fig. 1A<sub>2</sub>; Horner et al. 2004). Although this suture is not presently visible in any specimen of *S. osborni*, Brown (1912) indicated that the squamosals meet medially in this species also. In posterior view, the ventral margin of the parietal process is sinusoidal with the triangular dorsolateral corner of the exoccipital articulating ventrally. Extending ventrolaterally, the postquadrate process (paraoccipital process of the squamosal) flatly contacts the paraoccipital process of the exoccipital. The postquadrate process tapers distally, terminating short of the ventral tip of the paraoccipital process of the exoccipital. The quadrate cotylus is situated anterior to the postquadrate process and formed a synovial joint with the dorsal head of the quadrate (Horner et al. 2004). The cotylus is con-

strained anteriorly by a triangular prequadrate process that extends ventrally for a short distance along the anterior edge of the quadrate. The precotyloid fossa is best defined in adults; however, the posterodorsal margin remains indistinct as in *Saurolophus osborni*. This fossa is well defined in *Prosaurolophus* and *Gryposaurus* but is absent in *Edmontosaurus* (Gates and Sampson 2007). Anteriorly, the squamosal process of the postorbital contacts the postorbital process of the squamosal along a scarf joint that extends the length of both processes. At the posterior extent of this contact, two triangular prongs of the squamosal process of the postorbital are received within reciprocal depressions on the dorsal and lateral surfaces of the squamosal.

**Postorbital.**—The postorbital is identical in both species of *Saurolophus*. In lateral aspect, it is T-shaped in small individuals, and Y-shaped in larger individuals. The postorbital of *S. osborni* is also Y-shaped in adults, but small individuals are unknown. In dorsal view, the prefrontal process is medio-laterally wide, contacting the supraorbital (palpebral of Maryńska and Osmólska 1979) anteriorly, frontal anteromedially, and the parietal posteromedially. Its ventral surface is concave but not deeply excavated as it is in *Edmontosaurus* and possibly *Shantungosaurus* (Horner et al. 2004). The lateral (orbital) margin of the prefrontal process is ontogenetically variable: it is smooth in all except the largest adult (PIN 551/358) in which it is dorsoventrally thickened and ornamented by a series of ridges and grooves. The cylindrical squamosal process tapers posteriorly where it laps the lateral surface of the postorbital process of the squamosal. The anteroventrally-directed jugal process tapers ventrally forming an anteroposteriorly flattened surface that loosely overlies the postorbital process of the jugal. Medial to the jugal process, a divot on the underside of the postorbital housed the dorsal head of the laterosphenoid.

**Prefrontal-supraorbital complex.**—Maryńska and Osmólska (1979) demonstrated the ontogenetic fusion between the supraorbitals and prefrontal in *S. angustirostris*. There are two supraorbitals that form the anterodorsal orbital margin (Fig. 1). The anterior element (supraorbital I) is subrectangular and approximately twice as long as supraorbital II, which is tabular. The lateral (orbital) margins of both supraorbitals are coarsely striated in even the smallest specimens and are dorso-laterally flared. The suture between the supraorbitals is coarsely interdigitating in ZPAL MgD-1/159 but is closed and indistinct in the larger specimen, PIN 551/359. Medially, they fuse to the prefrontal early in ontogeny (the sutures are visible ventrally in ZPAL MgD-1/159 and PIN 551/359) along a straight suture that prevents them from contacting the nasal. Contact between the prefrontal-supraorbital complex and the postorbital excludes the frontal from the orbital rim. Bell (2011) identified two supraorbitals in *S. osborni* that conform to the configuration in *S. angustirostris*. Although the supraorbital-prefrontal suture cannot be observed in the holotype of *S. osborni* (AMNH 5220), the suture between supraorbitals I and II is observable ventral to the orbital rim. In *S. osborni*, the

lateral edges of the supraorbitals are upturned and sub-vertical compared to the relatively horizontally-lying supraorbitals in *S. angustirostris*. It is unclear whether this unusual condition in *S. osborni* is real or due to post-depositional deformation as it is only observable in the holotype; the supraorbitals are incomplete or not preserved in other specimens of *S. osborni*. Two supraorbitals are also present in *Maiasaura* (Horner 1983) and *Prosaurolophus* (Maryńska and Osmólska 1979).

The prefrontal is an elongate bone that lies parallel and ventral to the nasal. It is deepest laterally where it fuses with the supraorbitals. Anteriorly, an anteroventral process extends from the prefrontal ventral to the nasal and is braced ventrally by the anteroventral process of the frontal. The anterior limit of the prefrontal cannot be observed in any specimen but likely extended most of the length of the frontal platform. The anteroventral processes do not meet medially, but contribute to the lateral width of the frontal platform for the nasals. Posterodorsally, the prefrontal sends a sheet of bone (posterodorsal process of the prefrontal) along the underside of the lateral half of the nasal crest (Fig. 3). Along its medial edge it contacts the posterodorsal process of the frontal. In juveniles (ZPAL MgD-1/159, PIN 551/359), the posterodorsal process of the prefrontal is weakly developed, formed by the upturned anteromedial edge of the prefrontal (Fig. 6). The posterodorsal process is broken in all observed specimens but may have been up to half the length of the crest based on the grooved pattern on the underside of the nasals. The suture between the prefrontal and nasal is loose even in the largest skulls (Maryńska and Osmólska 1981). Brown (1912) suggested the posterodorsal process in *S. osborni* fuses distally with the nasal; however, this could not be confirmed from the current mount of the holotype (Bell 2011). Only the base of this process is observable in *S. osborni* (CMN 8796), where it conforms to the morphology described for *S. angustirostris*.

**Lacrimal.**—The outline of the lacrimal forms an isosceles triangle; the short side comprises part of the anterior orbital rim. In adults, the anterior tip reaches a point level with and ventral to the posterior margin of the external narial opening, although in juveniles it is dorsal and posterior to the naris. The dorsal apex is partially enclosed by supraorbital I in a loose bridle joint. The anterodorsal edge contacts the nasal along its length and, superficially, the lateral process of the premaxilla. Complete overlap by the posterolateral process of the premaxilla also occurs in *S. osborni* and *Brachylophosaurus* (Cuthbertson and Holmes 2010). However, the posterolateral process is shorter in *Gryposaurus* (Gates and Sampson 2007), *Prosaurolophus* (CMN 2277, ROM 1928), and *Edmontosaurus* (CMN 2288, CMN 8509), and incompletely overlaps the lacrimal. Ventrally, the lacrimal contacts the jugal posteriorly and the maxilla for a short distance anteriorly. The relative length of the lacrimal-maxilla contact increases with skull length. The general shape of the lacrimal is closest to *S. osborni* and *Prosaurolophus*, but is similar also to *Maiasaura* (Horner 1983) and *Brachylophosaurus* (Prieto-Marquez 2005).

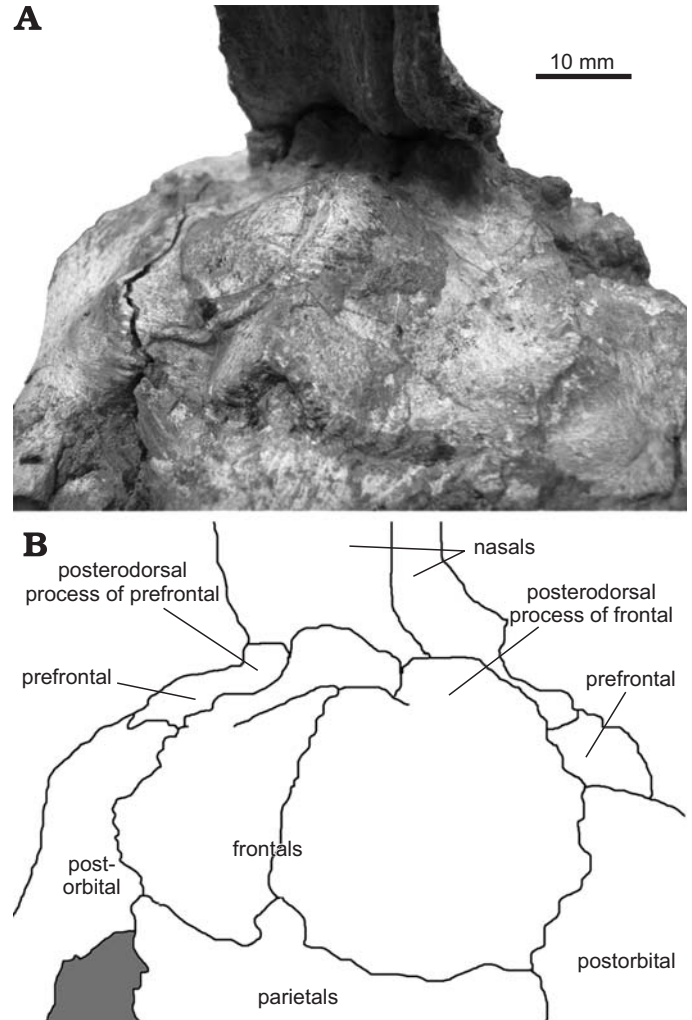


Fig. 6. Dorsal oblique view of juvenile *Saurolophus angustirostris* Rozhdestvensky, 1952, ZPAL MgD-1/159, late Campanian–?Maastrichtian Nemegt Formation, Mongolia; skull roof. Photograph (A) and explanatory drawing (B). Shading indicates matrix.

## Neurocranial complex

**Frontal.**—Each frontal is tripartite, consisting of a frontal body, an anteroventral process, and a posterodorsal process. In dorsal view, the frontal body is trapezoidal and flat lying in adults (Maryńska and Osmólska 1981). In juveniles, they are semicircular and domed (Fig. 6). Doming of the frontals is typical of adult lambeosaurines but is present also in *Lophorhynchon* (Horner et al. 2004). Juvenile *S. osborni* are unknown, but the frontals are flat in adults. The frontal body is bounded posteriorly by the parietal, laterally by the postorbital, and anterolaterally by the prefrontal. Contact between the postorbital and prefrontal excludes the frontal from the orbital rim as in *S. osborni*, *Prosaurolophus* (CMN 2277, ROM 1928) and Lambeosaurinae. Ventrally, the cerebral cavity occupies the posteromedial quadrant of the frontal. This cavity is bounded anterolaterally by the presphenoid and posteriorly by the orbitosphenoid and laterosphenoid.

The cerebral cavity narrows anteriorly for the passage of cranial nerve I. Lateral to the presphenoid contact, the orbital cavity continues as a shallow depression on the ventrolateral surface of the frontal body. The anteroventral process of the frontal is trapezoidal in anterior view and forms a platform that underlies the prefrontal and nasal. The surface of the frontal platform is smooth, forming a weak contact between these elements. Anteromedially, the frontal platform continues posterodorsally as a strap-like posterodorsal process, which underlies the nasal crest (Fig. 3). Proximally, this process is buttressed along its lateral edge; elsewhere it is thin and usually broken even in well-preserved specimens. It extends approximately half the length of the crest in large animals. In juvenile specimens (ZPAL MgD-1/159, PIN 551/359), the posterodorsal process forms a blunt stub (contra Maryańska and Osmólska 1979, 1981) similar to that observed on juvenile *Parasaurolophus* (Fig. 6; Evans et al. 2007). This short process terminates within a depression on the underside of the nasal. As adults, however, the elongate posterodorsal process lies within a corresponding groove on the underside of the nasal. Contact between neighbouring posterodorsal processes is prevented in all specimens by a median ridge formed by the paired nasals. The short description of the posterodorsal process in *S. osborni* by Brown (1912) complies with that of *S. angustirostris*; however, it cannot be adequately observed in the holotype. In CMN 8796, the incompletely-preserved posterodorsal process is a finger-like process that is about as long as the frontal contribution to the skull roof. The preserved portion is equivalent in position and morphology to the lateral buttress on the posterodorsal process of *S. angustirostris*.

**Parietals.**—Work by Horner and Currie (1994) shows that the hadrosaurid parietals form a single median element through the fusion of two embryonic elements. The parietals form a median, saddle-shaped element that defines the medial borders of the supratemporal fenestrae. The parietals are widest anteriorly where they contact the frontals anteriorly and post-orbitals anterolaterally. A shallow triangular depression is present dorsally on the anterior half of the parietals. A medial spur separates the frontals at their posteromedial border (Figs. 1, 6). This spur is wedge-shaped in ZPAL MgD 1/159, but is virtually absent in PIN 551-359. This spur is also wedge-shaped in *Prosaurolophus* (Horner 1992, CMN 2277), and finger like in *Edmontosaurus* (AMNH 427, CMN 8509). It cannot be observed in *S. osborni* due to damage. In most hadrosaurines (except *Brachylophosaurus* [CMN 8893] and *S. osborni*), the parietals and frontals are flat-lying in lateral view. In *S. angustirostris*, the angle between these elements becomes more acute with age. The posterior two-thirds of the length of the parietals are mediolaterally constricted and form a sagittal crest, which becomes progressively taller in older animals. A tall sagittal keel and acute angle between the frontals and parietals are unique to *Saurolophus* spp. and Lambeosaurinae (Bell 2011). The sagittal crest posteriorly contacts the parietal processes of the squamosals, which exclude it from

the posterior border of the skull. Ventrally, the parietals enclose the dorsal half of the cerebral cavity and are bounded anterolaterally by the laterosphenoid and presumably by the supraoccipital posterolaterally, although the latter cannot be seen in complete specimens.

**Otoccipital.**—The exoccipital fuses with the opisthotic early in embryonic development (Horner and Currie 1994) forming a single element, the otoccipital. Together with the supraoccipital, the otoccipital forms the dorsal and lateral parts of the occiput. Ventrally, the club-like basioccipital process abuts the basioccipital to form the hemispherical occipital condyle. This union is dorsomedially inclined. In PIN 551/359, the basioccipital processes do not meet ventrally; a narrow portion of the basioccipital completes the circumference of the foramen magnum. This is true for all hadrosaurines except *P. blackfeetensis*, where the basioccipital is apparently excluded from the foramen magnum (Horner 1992). In all other specimens of *S. angustirostris*, this relationship is obscured by fusion or diagenetic deformation.

Posterior to the crista tuberalis, three foramina penetrate the lateral wall of the basioccipital process in a sub-horizontal line. The posterior two correspond to the hypoglossal nerve (XII). The more anterior opening converges medially with a tract that exits laterally anterior to the crista tuberalis. Together they form a fossa on the medial wall of the otoccipital that housed the common root of cranial nerves IX, X, and XI (Fig. 7B). It is therefore equivocal whether cranial nerve X exited anteriorly with cranial nerve IX or posteriorly with the accessory nerve. The crista tuberalis extends anteroventrally onto the lateral face of the basioccipital, and posterodorsally, where it is continuous with the ventral margin of the paroccipital process. Anterior to the opening for cranial nerve IX, the fenestra ovalis opens medially into a spherical vacuity (otic vestibule) formed by the otoccipital and prootic (Fig. 7).

In posterior view, the paroccipital process extends dorso-laterally above the level of the supraoccipital before turning ventrolaterally and tapering to a rounded tip. The ventral limit of the paroccipital process is approximately level with the base of the basioccipital process, similar to the condition in *S. osborni* (AMNH 5221), *Gryposaurus* (Gates and Sampson 2007), and *Prosaurolophus* (CMN 2277; Horner 1992). The otoccipitals contact medially ventral to the supraoccipital along a straight, vertical suture that is visible as a low ridge in some specimens. Anteromedially, the exoccipital has a finely-ridged sutural contact with the supraoccipital. These ridges are parallel and angled ventromedially.

**Supraoccipital.**—With the exoccipitals, the unpaired supraoccipital forms the dorsal margin of the occiput. In posterior view, it forms a trapezoidal bar ventral to the dorsal-most point of the exoccipitals, to which it is fused. The dorsal margin is concave. As it is only known from articulated complete specimens, the internal morphology of the supraoccipital is unknown. The supraoccipital is not observable in any specimen of *S. osborni*.

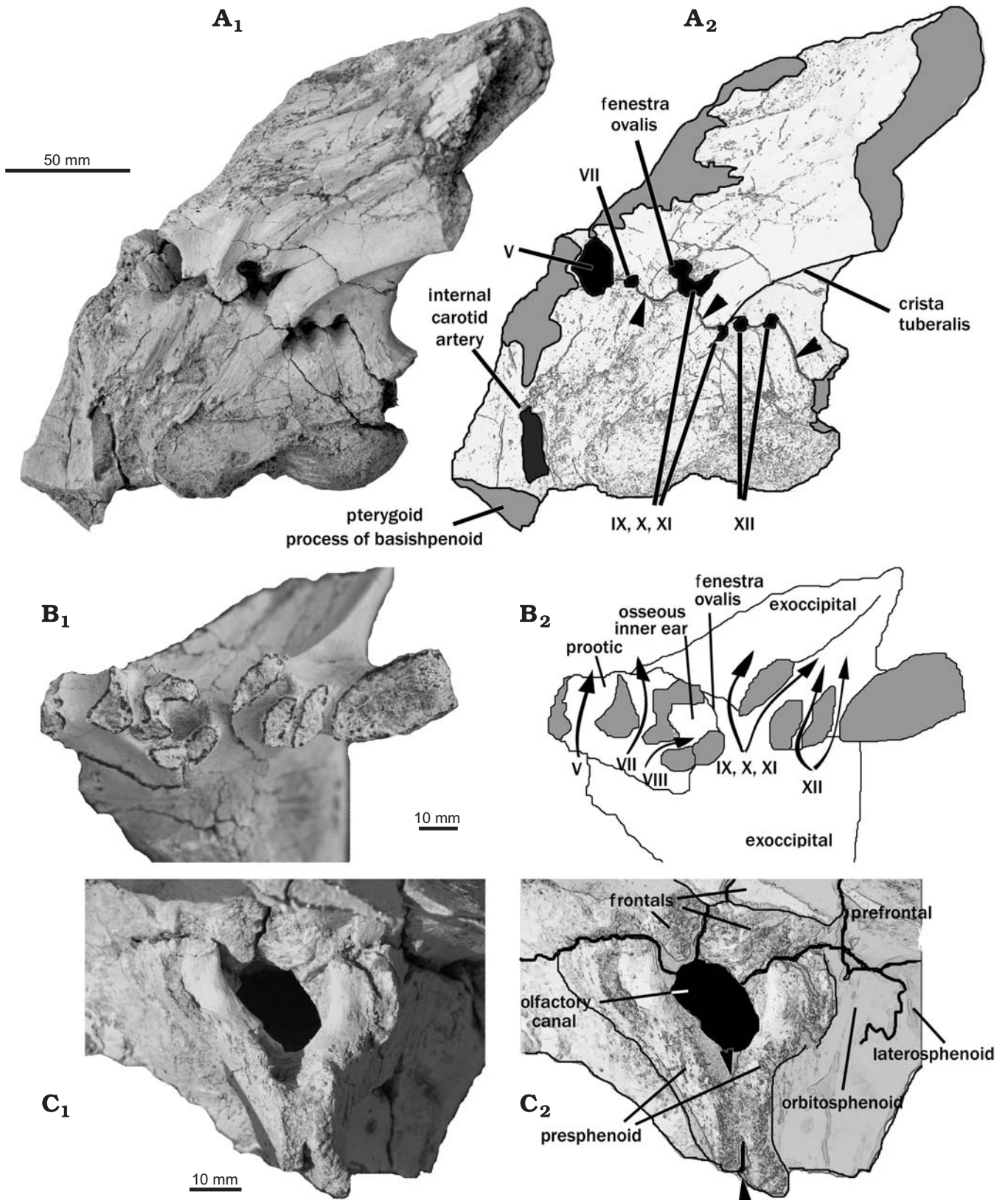


Fig. 7. Partial braincase of adult hadrosaurid dinosaur *Saurolophus angustirostris* Rozhdestvensky, 1952, KID 476, late Campanian–?Maastrichtian Nemegt Formation, Mongolia. **A**. Left lateral view of otoccipital, basioccipital, prootic, and basisphenoid. **B**. Ventral view of left otoccipital and prootic across broken surface denoted by arrowheads in **A**<sub>1</sub>. **C**. Anterior view of braincase showing the paired presphenoids. The inter-presphenoid suture is indicated by arrowheads. Grey regions indicate broken surfaces. Cranial nerves are indicated with roman numerals. Photographs (**A**<sub>1</sub>, **B**<sub>1</sub>, **C**<sub>1</sub>) and explanatory drawings (**A**<sub>2</sub>, **B**<sub>2</sub>, **C**<sub>2</sub>).

**Basioccipital.**—Posteriorly, the convex margin of the unpaired basioccipital forms the ventral half of the occipital condyle. It is differentiated from the rest of the element ventrally by a transverse sulcus that is present in most hadrosaurines except *Brachylophosaurus* where it is variably present (Gates and Sampson 2007; Cuthbertson and Holmes 2010). Anterior to this sulcus, the basioccipital swells to meet the basisphenoid along a rugose, closed suture. Together, these elements form the paired basitubera, which are separated by a medial furrow. Dorsolaterally, the basioccipital contacts the otoccipital for most of its length. A contact with the prootic was likely present anterolaterally, although fusion has obscured this suture. Dorsally, a longitudinal furrow marks the position of the medulla. The basioccipital forms a minor part of the ventral margin of the foramen magnum but does not appear to participate in the formation of any additional cranial nerve foramina.

**Basisphenoid.**—The basisphenoid fuses anteriorly with the parasphenoid early in embryonic development to form a single element (Horner and Currie 1994). It fuses posteriorly with the basioccipital and dorsally (from anterior to posterior) with the presphenoid, laterosphenoid, and prootic. Between the presphenoid and laterosphenoid contacts, it forms the ventral part of a large neurovascular foramen. Maryańska and Osmólska (1981) suggested that cranial nerves III and VI exited via this foramen; however, in PIN 551/359 the foramen for cranial nerve III is visible as a distinct foramen on the laterosphenoid dorsal to the opening for the abducens nerve (CN VI; Fig. 8). In *S. osborni*, the foramina for cranial nerve III and VI are also separate and a distinct groove extends anteriorly from the foramen for cranial nerve III. In anteroventral aspect, the basisphenoid is triangular. The anterior apex of the basisphenoid extends to form the blade-like parasphenoid process (cultriform process). In lateral view, the parasphenoid process extends anteriorly and tapers to a point that terminates anterior to the presphenoid. This process is mediolaterally widest dorsally although it could not be determined if it is also dorsally concave as it is in *Brachylophosaurus* and *Maiasaura* (Prieto-Marquez 2005). Dorsally, at the base of this process, the median palatine artery emerged along a shallow, horizontal cleft between the basisphenoid and presphenoid. The pterygoid processes diverge posteroventrally from the posterolateral corners of the basisphenoid. Each finger-like pterygoid process ends in the angle formed by the quadrate process and basisphenoid process of the pterygoid. There is no medial prong on the transverse ridge that separates these processes; a condition shared only with *S. osborni* and *Prosaurolophus* (Gates and Sampson 2007). Just posterior to the base of each pterygoid process, a dorsoventral groove becomes the opening for the interior carotid artery (Figs. 7A, 8). This passageway extends dorso-medially and opens into the pituitary (hypophyseal) fossa. Within the pituitary fossa, dorsal to the foramina for the internal carotids and ventral to the dorsum sellae, a pair of smaller foramina marks the passage of cranial nerve VI.

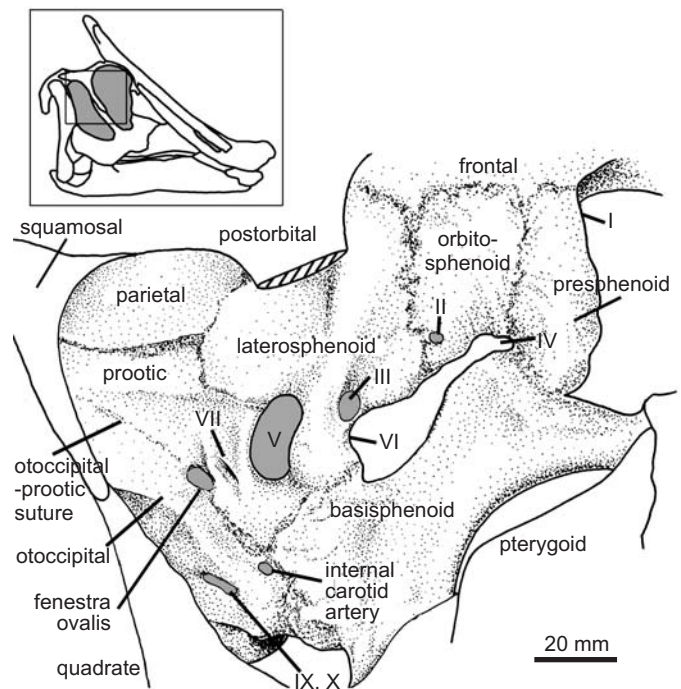


Fig. 8. Hadrosaurid dinosaur *Saurolophus angustirostris* Rozhddestvensky, 1952, PIN 551/359, late Campanian–?Maastrichtian Nemegt Formation, Mongolia. Right lateral view of juvenile braincase with postorbital and jugal processes removed (cross hatching). Enlarged area demarcated by boxed area on inset. Grey regions denote neurovascular openings.

These passageways extend posterodorsally emerging onto the floor of the endocranial cavity.

**Laterosphenoid.**—The laterosphenoid is dorsoventrally elongate, with its dorsal terminus inserting into a cotylus on the ventral surface of the postorbital. The laterosphenoid extends ventrally to meet the basisphenoid posterior to the foramen for cranial nerve VI. The anterior contact with the orbitosphenoid is interdigitating in PIN 551/8, but is obliterated by fusion in MPC 100/706. Posteriorly, the laterosphenoid encloses the anterior margin of the foramen for cranial nerve V to exclude the basisphenoid from participating in the formation of that foramen. A tabular posterior extension of the laterosphenoid is present immediately dorsal to this foramen (Fig. 8), as in *Brachylophosaurus*, *Gryposaurus*, and *Prosaurolophus* (Gates and Sampson 2007), which contacts the parietal posterodorsally and the prootic posteroventrally. A ridge in this region in *S. osborni* may indicate a similar posterior extension of the laterosphenoid, but in most cases, fusion with the prootic makes interpretation difficult. This posterior extension is visible in PIN 551/357, but is indistinct in larger specimens due to fusion with the prootic. The ophthalmic branch of cranial nerve V lay in a longitudinal sulcus that separates the subcircular preotic pendant (alar process sensu Horner et al. 2004) from the rest of the laterosphenoid. The preotic pendant is appressed to the surface of the laterosphenoid and not wing-like as it is in *Brachylophosaurus* (Cuthbertson and Holmes 2010). The laterosphenoid

of *S. osborni* is firmly co-ossified with the surrounding elements, hence its margins cannot be discerned.

**Prootic.**—The prootic is best seen in PIN 551/359 and MPC 100/706. The anterior margin is invaginated at its mid-height to form most of the circumference of the foramen for the large trigeminal nerve (cranial nerve V). Dorsal to that foramen, the prootic forms an elongate triangle, the dorsal margin of which contacts the parietal. The posterior margin of the prootic is roughly parallel to the crista tuberalis but is visible only in PIN 551/357 (Fig. 8); it is indistinguishably fused with the otoccipital in MPC 100/706. The prootic contacts the basisphenoid ventral to the trigeminal foramen. Posteriorly, the prootic contacts the otoccipital and basioccipital ventrally. Along with the opisthotic, the prootic forms the fenestra ovalis and the anterior half of the otic vestibule. Cranial nerve VIII entered the otic vestibule from the medial wall of the prootic as in *Prosaurolophus* (Figs. 7B; Horner 1992). The small foramen for cranial nerve VII is between the fenestra ovalis and the trigeminal nerve foramen. In PIN 551/359, separate grooves for the palatine and hyomandibular branches extend ventrally and dorsally, respectively, from the foramen for the trigeminal nerve. In KID 476, however, the palatine branch groove is faint and that for the hypoglossal branch is absent altogether, as in *S. osborni* (AMNH 5221). Separating the position of cranial nerve VII from the fenestra ovalis is a ridge, the crista preotica. In PIN 551/359 the crista preotica is short, but in MPC 100/706 it extends posterodorsally to join the more robust crista prootica. The crista prootica is nearly horizontal, extending the anteroposterior length of the prootic onto the lateral face of the otoccipital. In *S. osborni*, the prootic is fused to other elements of the lateral wall of the braincase, hence its general outline is unknown. The other features do not differ from *S. angustirostris*.

**Presphenoid.**—There is doubt regarding the identification and homology of the presphenoid in hadrosaurids (Evans 2006; Ali et al. 2008; McBratney-Owen 2008). Nevertheless, “presphenoid” (= sphenethmoid in non-avian theropods, Ali et al. 2008) is used here for consistency in the hadrosaurid literature. The presphenoids are paired ossifications that together form a Y-shaped element in anterior view, attaching dorsally to the ventral surfaces of the frontals (Fig. 7C). The U-shaped dorsal component forms the canal for the olfactory bulbs and nerve (cranial nerve I). Ventral to this canal, the presphenoids meet to form the “interorbital septum”. In lateral aspect, the presphenoid is roughly quadrangular in PIN 551/359, contacting the orbitosphenoid posteriorly and the basisphenoid posteroventrally as in *S. osborni* and *Prosaurolophus* (Horner 1992), but not *Brachylophosaurus* (Prieto-Marquez 2005). Anteroventrally, a cleft separates the presphenoid from the basisphenoid and transmitted the median palatine artery. The posteroventral margin of the presphenoid forms the anterior half of the foramen for cranial nerve IV (Fig. 8). This foramen is closed posteriorly by the orbitosphenoid.

**Orbitosphenoid.**—The orbitosphenoid is a dorsoventrally tall, ovoid element. It is surrounded by the presphenoid anteriorly, the frontal dorsally, and the laterosphenoid posteriorly. Ventrally, it forms part of the dorsal wall for the antero-posteriorly elongate neurovascular foramen that included cranial nerve VI (Maryńska and Osmólska 1981). This fenestra separates the orbitosphenoid from the basisphenoid (Fig. 8). Posteroventrally, the orbitosphenoid is perforated by the foramen for cranial nerve II. A groove for that nerve extends anteriorly from the optic foramen. In most cases the anteroventral margin of the orbitosphenoid forms the posterior margin of the foramen for the fourth cranial nerve. However, this foramen is not entirely enclosed posteriorly in PIN 551/359, and as a result, forms the anterior margin of the elongate neurovascular foramen that includes the foramen for cranial nerve VI (Fig. 8).

### Palatal complex

The palatal bones are known only in complete specimens in which they are visible through the orbits and temporal fenestrae. Their complete morphology and relationships are therefore incompletely known. The strongly vaulted palate of ZPAL MgD-1/159 (Maryńska and Osmólska 1981) is the result of crushing. It is a broadly arcing complex consistent with other hadrosaurines (Heaton 1972).

Posteriorly, the pterygoid is loosely adhered to the medial surface of the pterygoid process of the quadrate. The dorsal quadrate process is triangular and posterodorsolaterally directed. The posteriorly directed ventral quadrate process is shorter and buttressed along its medial surface. Antero-dorsally, the broad palatine process extends to meet the posterior margin of the palatine and medially to contact its counterpart. Together, the palatine processes form a vaulted palate typical of hadrosaurines; in contrast, the lambeosaurine palate is more steeply vaulted (Heaton 1972). The dorsal margin of the palatine process originates proximally on the medial surface of the dorsal quadrate process. At this contact, they form a deep sulcus that houses the pterygoid process of the basisphenoid (Fig. 1A<sub>2</sub>). The ectopterygoid process is strongly buttressed, extending ventrally to contact the posterior edge of the maxilla. The ectopterygoid partially overlaps the lateral surface of this process.

Part of the ectopterygoid is observable through the orbit of ZPAL MgD-1/159, as illustrated by Maryńska and Osmólska (1981: fig. 5). It extends, strap-like, along the posteroventral margin of the palatine, the ventrolateral surface of the palatine process of the pterygoid and the lateral surface of the ectopterygoid process of the pterygoid.

Anteroventrally, the palatine is mediolaterally expanded to contact the posteromedial surface of the anterior process of the jugal. The main body of the palatine rises dorsally into the interorbital cavity to form a blade-like extension that contacts its mate medially. The anterior edge is concave. In most hadrosaurines, the dorsal margin of this extension flares anteroposteriorly in lateral view; however, it tapers in

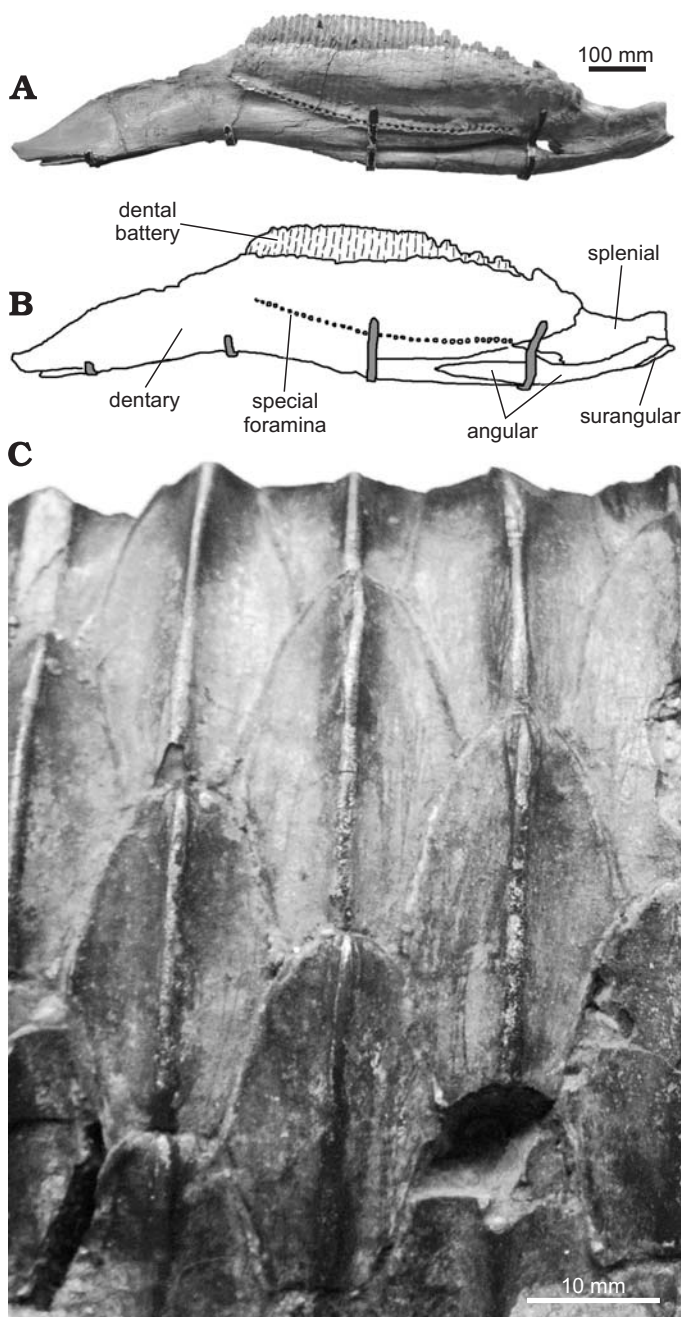


Fig. 9. Right dentary of hadrosaurid dinosaur *Saurolophus angustirostris* Rozhdstvensky, 1952, PIN 551/407, late Campanian–?Maastrichtian Nemegt Formation, Mongolia. **A.** Right dentary in lingual view. **B.** Explanatory drawing of the same. **C.** Lingual view of dentary teeth from the middle of the tooth row.

*Saurolophus angustirostris* and possibly *S. osborni* (Heaton 1972). The palatine meets the pterygoid posteriorly. Ventrally, the contact with the maxilla is obscured by the ectopterygoid.

The dorsal apex of the vomer is visible in ZPAL MgD-1/159 just anterior to the palatine. At this point, the vomers are united and extend posteriorly between the paired palatines. Anteriorly, they are obscured by the nasals.

## Mandibular complex

The single, median prementary is a horseshoe-shaped element that wraps around the mandibular symphysis. The postero-lateral processes are dorsoventrally flattened and taper posteriorly. In MPC 100/706, the terminus is bifurcated. The postero-medial surface of the prementary has a dorsally placed triangular process and more ventrally placed paired, tabular processes, both of which enclose the dental symphysis above and below, respectively. The oral margin is smooth in young animals, becoming slightly more irregular in later ontogeny. It is perforated by five or six foramina on either side of the midline.

In lateral view, the dentary is straight along its ventral edge (Fig. 9A) as in *S. osborni*, *Prosaurolophus* (e.g., CMN 2277, ROM 1928), and *Edmontosaurus* (CMN 2288, CMN 8509). The robust, distally-expanded coronoid process is procumbent and inserts into a space (adductor chamber) medial to the jugal. Medially, the dental battery is covered by a thin plate of bone (dental lamina) that is perforated by a row of special foramina (Edmund 1957). Each foramen corresponds to the base of a vertical tooth family and together they form a concave arc. Posterior to the dental battery, the dentary has a subconical process that contacts the lateral surface of the splenial. The splenial process is separated from the lateral wall of the dentary by a cleft (Meckelian fossa) that extends anteroventrally and forms the contact for the angular. The edentulous portion of the dentary constitutes 40% of the length of the dentary (irrespective of dentary length) and tapers anteriorly. The symphyseal region is offset medially and ventrally from the main body of the dentary, where it loosely abuts its neighbour. A vascular foramen exits anteroventrally near the symphysis and several smaller foramina open onto the lateral surface of the dentary.

The dentary houses at least 26 vertical tooth families in ZPAL MgD-1/159 and 50 in PIN 551/407. A high tooth count (>46 families) characterises *Edmontosaurus* and species of *Saurolophus*, but is linked to both ontogeny and absolute size. Up to six teeth are present within a single tooth family, although only one or two are functional for mastication at any one time. The enamelled lingual surface is diamond shaped with a single, straight median carina. The teeth are typically hadrosaurine, being relatively short with a crown height that is close to twice the mesiodistal length. Marginal denticles are present only on the anterior-most teeth and are absent or poorly developed posteriorly (Fig. 9B).

The largest element in the postdentary complex (Bell et al. 2009) is the surangular, which is U-shaped in lateral view. The dorsal surface is mediolaterally flared and excavated to receive the ventral condyles of the quadrate. A triangular process on the dorsolateral edge of the surangular restricts lateral movement in the jaw joint between the quadrate and the surangular. Posteriorly, the surangular is mediolaterally compressed; it contacts the articular medially. Anteriorly, the coronoid process of the surangular is thin and triangular and resides along the medial surface of the lateral wall of the den-

tary. The surangular contacts the angular ventromedially and the splenial medially.

The angular is straplike and forms the ventral edge of the postdentary complex (Fig. 9A). It extends anteriorly along the ventromedial surface of the dentary, where it is housed within a cleft. Posteriorly, it is contacted by the splenial dorsally and the surangular medially. The posterior half of the angular, in ventral aspect, is sinusoidal.

The splenial is a thin, subrectangular plate on the medial surface of the postdentary complex (Fig. 9A). It tapers posteriorly and contacts the angular ventrally and articular posterolaterally. The dorsal edge of the splenial is concave where it contacts the articular. Anteromedially, a V-shaped depression receives the corresponding splenial process of the dentary.

Wedged between the posterior ends of the surangular and splenial is the articular. The articular is a vertically-oriented ovate element that forms a part of the articulating surface of the jaw joint for the quadrate. In medial view, the dorsal half of this element is visible dorsal to the splenial, but is almost entirely obscured by the surangular in lateral aspect.

### Accessory elements

**Sclerotic ring.**—Three to five sclerotic plates, none of which is complete, are preserved in the right orbit of PIN 551/8 (Fig. 10). Three are in situ and the other two are broken and displaced. As preserved, these conform to the posterodorsal quadrant of the sclerotic ring. The plates are serially overlapping in an anti-clockwise direction; the posterior edge of a plate overlaps the leading edge of the following plate. The edges of the individual plates are finely crenulated, with the exception of the inner (i.e., toward the centre of the ring) margin, which is smooth. The overlapping portion is lobate (compared to the triangular processes in other hadrosaurids; Russell 1940; Ostrom 1961); however, the edges are incomplete. No plus or minus plates (sensu Lemmrich 1931) could be identified from the limited sample. Brown (1912) posited that the sclerotic plates in *S. osborni* were entirely serially overlapping; however, as pointed out by Russell (1940), this would be a unique arrangement. Reanalysis of the holotype AMNH 5220 confirms Russell's (1940) suspicions. The anterodorsal quadrant is composed of three serially overlapping plates in an anti-clockwise direction, where the triangular trailing edge of a plate is received in a reciprocal facet on the following plate. In the anteriormost plate, that facet is visible where the preceding plate has become displaced. The adjacent, displaced plate lacks facets on its lateral surface, identifying it as a plus plate. A minus plate is present at the other end of the three aforementioned serially overlapping plates. If correct, this would confirm previous interpretations of a Lemmrich type A arrangement in *Saurolophus* (Russell 1940; Ostrom 1961).

**Hyoid.**—The hyoid is visible only in the adult specimen PIN 551/357. It is rod-like, measuring 450 mm long and 90 mm high at the proximal (anterior) end. The proximal end is flattened and is triangular in cross-section. Each side of the trian-

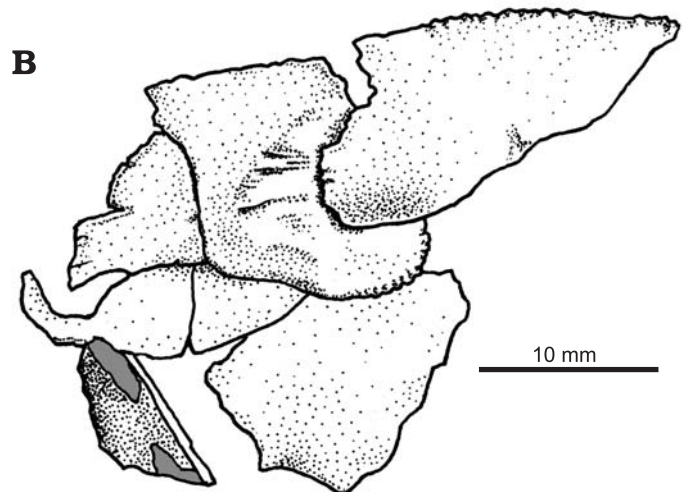


Fig. 10. Partial sclerotic ring within right orbit of hadrosaurid dinosaur *Saurolophus angustirostris* Rozhdestvensky, 1952, PIN 551/8, late Campanian–?Maastrichtian Nemegt Formation, Mongolia. Photograph (A), explanatory drawing (B). Grey regions in B denote matrix. Dorsal is up.

gle is concave and the shortest side is situated ventrally. The hyoid tapers gradually from the proximal end, becoming elliptical in cross-section. The hyoid is straight except for the distal third, which is offset posterodorsally. Left and right hyoids converge anteriorly at the ventromedial corner of their proximal ends. This convergence point is approximately ventral to the basisphenoid.

### Phylogenetic analysis

The purpose of this analysis was to assess the position of *S. angustirostris* relative to *S. osborni*, rather than to comprehensively test the interrelationships of Hadrosaurinae as a whole. Forty-four cranial characters, as compiled from Weishampel et al. (1993), Godefroit et al. (2008), Bolotsky and Godefroit

Table 2. Character-taxon matrix for phylogenetic analysis performed in this study. Character numbers and definitions correspond to those provided by Bell (2011).

|                                   | 1–5   | 6–10  | 11–15 | 16–20 | 21–25 | 26–30 | 31–35 | 36–40 | 41–44 |
|-----------------------------------|-------|-------|-------|-------|-------|-------|-------|-------|-------|
| <i>Iguanodon</i>                  | 00000 | 00000 | 00000 | 00000 | 00000 | 00000 | 00000 | 00000 | 0000  |
| <i>Bactrosaurus</i>               | 00000 | 00000 | 00000 | 00000 | 00000 | 00000 | 00000 | 00000 | 0000  |
| <i>Lambeosaurus</i>               | 01011 | 11110 | 10110 | 20110 | 11101 | 00011 | 10111 | 21111 | 1211  |
| <i>Hypacrosaurus</i>              | 01011 | 11110 | 10110 | 20120 | 11101 | 00011 | 10111 | 21111 | 1211  |
| <i>Maiasaura</i>                  | 00100 | 00011 | 01000 | 01002 | 10011 | 00012 | 21110 | 01111 | 2210  |
| <i>Brachylophosaurus</i>          | 00100 | 00011 | 01001 | 01201 | 10011 | 00012 | 21110 | 11121 | 2210  |
| <i>Gryposaurus</i>                | 00100 | 00012 | 01001 | 01000 | 10001 | 10013 | 11110 | 01111 | 1210  |
| <i>Kerberosaurus</i>              | 001?1 | 000?? | ????? | ?2??0 | 10001 | ?013  | 11110 | ?11?? | ?2?0  |
| <i>Prosaurolophus</i>             | 00101 | 00012 | 01001 | 12001 | 10001 | 10013 | 11110 | 01121 | 1210  |
| <i>Edmontosaurus</i>              | 00100 | 00013 | 01001 | 12000 | 10001 | 11013 | 11110 | 21131 | 1310  |
| <i>Saurolophus osborni</i>        | 10111 | 02212 | 01001 | 12202 | 1210? | ?0013 | 11110 | 01121 | ?210  |
| <i>Saurolophus angustirostris</i> | 10111 | 02202 | 01001 | 12202 | 12101 | 10013 | 111?0 | 01121 | 1310  |

(2004), Horner et al. (2004), Prieto-Marquez (2005), and modified by Bell (2011) were used to evaluate the phylogenetic position of *Saurolophus angustirostris* (Table 2). Character numbers and descriptions correspond to those in Bell (2011). Ten ingroup and two outgroup taxa (*Iguanodon* and *Bactrosaurus*) were scored, with all characters assigned equal weight and unordered. A heuristic search using parsimony with 1000 random addition sequence replicates performed using PAUP 4.0b10 (Swofford 2002) retrieved three most parsimonious trees with a length of 72 steps. These differed only in the relationships of *Kerberosaurus* and *Prosaurolophus* to *Saurolophus* spp. In the strict consensus tree (Fig. 11), these three genera form a polytomy; however, *S. angustirostris* is recovered as the sister taxon of *S. osborni*, confirming the simi-

ilarity between these two species. *Saurolophus* is strongly united by the following unambiguous synapomorphies: a parietal that is excluded from the posterodorsal margin of the occiput by the squamosal (Character 1); secondary elongation of the frontal resulting in the backwards extension of the frontal platform (Character 7); a frontal platform that extends dorsal to the anterior portion of the supratemporal fenestra (Character 8); and a prefrontal that participates in the ventrolateral portion of the crest (Character 22). *Kerberosaurus*, *Prosaurolophus*, and *Saurolophus* are weakly united by one ambiguous character (frontal excluded from the orbital rim by the post-orbital-prefrontal union; Character 5). General topology agrees well with those of Bolotsky and Godefroit (2004) and Godefroit et al. (2008) except that the current analysis recovered *Kerberosaurus*, *Prosaurolophus*, and *Saurolophus* in a polytomy. *Kerberosaurus* is the sister taxon to a clade that includes *Prosaurolophus* and *Saurolophus* in the analyses of Bolotsky and Godefroit (2004) and Godefroit et al. (2008). The only previous study to incorporate both species of *Saurolophus* in a phylogenetic analysis is that of Prieto-Marquez (2010). Although the current analysis is limited in terms of both taxa and cranial characters (compared to the extensive list of cranial and postcranial characters used by Prieto-Marquez 2010), both studies recovered a monophyletic *Saurolophus* clade; however, Prieto-Marquez (2010) also resolved *Kerberosaurus* as the sister taxon to the clade comprising *Saurolophus* and *Prosaurolophus*.

## Discussion

The most characteristic feature of the skull in *Saurolophus* is the nasal crest and the involvement of the prefrontals and frontals in its construction. Although a posterodorsal process of the frontal was described for *S. osborni* by Brown (1912), the inaccessibility of the mount led to doubt of its existence (Ostrom 1961; Horner 1992; Horner et al. 2004). The absence of a posterodorsal process of the frontal was used by Horner (1992) to differentiate *S. osborni* from *S. angustiro-*

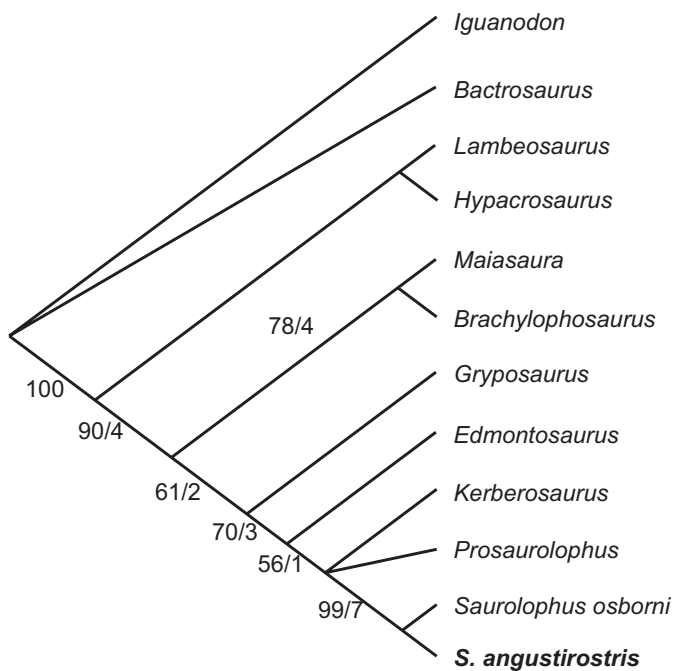


Fig. 11. Strict consensus tree showing the phylogenetic position of *Saurolophus angustirostris* Rozhdestvensky, 1952. RI = 0.87, CI = 0.84, and RCI = 0.74. Values at the base of nodes refer to bootstrap and decay indices, respectively.

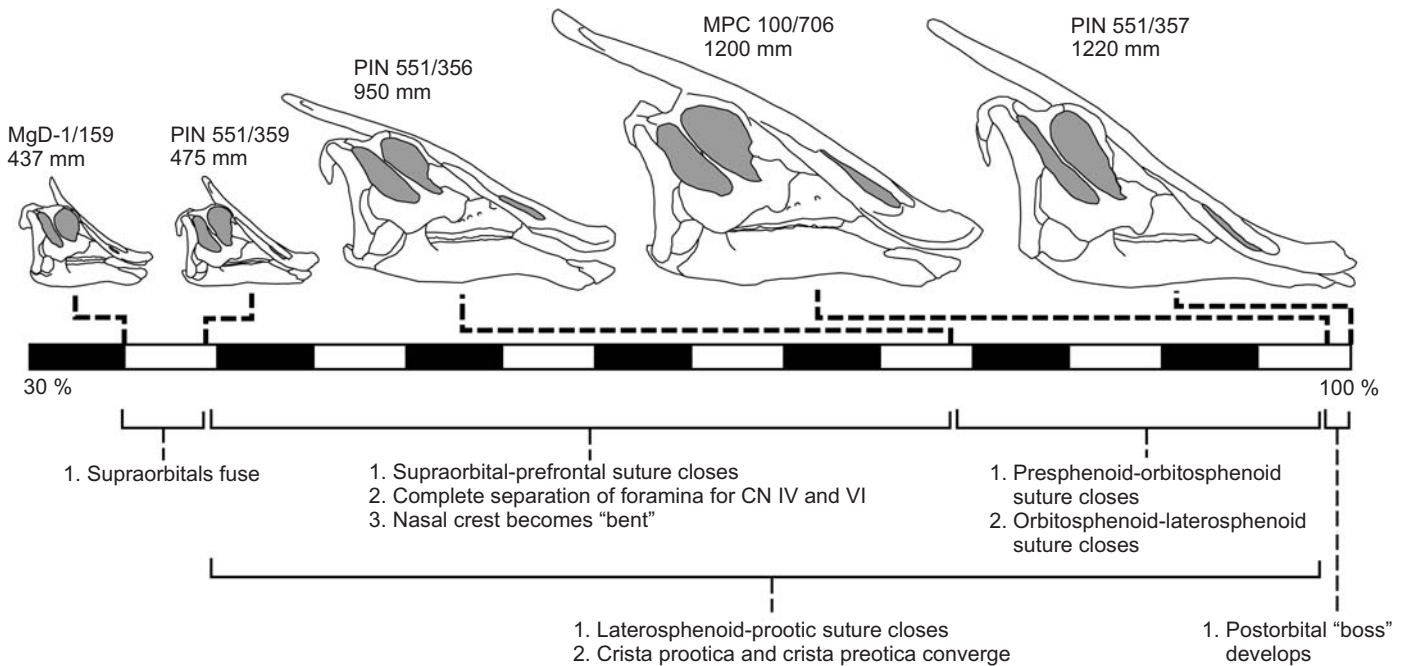


Fig. 12. Ontogenetic series of *Saurolophus angustirostris* Rozhdestvensky, 1952 skulls (late Campanian–?Maastrichtian Nemegt Formation, Mongolia) with associated neurocranial (and select dermatocranial) changes. Specimens are placed on the scale bar as a percentage of length of the largest specimen. Specimens are to scale.

rostris; however, Bell (2011) has demonstrated its presence in both species. Brown (1912: 135) described this process in the holotype of *S. osborni* as “broad”; however, in the only specimen where it is currently observable (CMN 8796), it is broken and forms a short, nearly conical spike that matches the equivalent region in *S. angustirostris*. Maryńska and Osmólska (1981) also suggested the posterodorsal process of the prefrontal may be relatively longer in *S. osborni*, but this cannot be demonstrated given that the crest is incomplete in all specimens of that species. Regardless, the prefrontal-frontal contribution to the crest in *Saurolophus* is peculiar among hadrosaurines. In other crested hadrosaurines, the prefrontals and frontals are not simultaneously involved in supporting the crest. In *Maiasaura*, however, where the frontals contribute to the crest, they extend dorsally to form a transverse, anterodorsally-inclined ridge that forms the posterior and dorsal parts of the crest (Horner 1983). Similar to most lambeosaurines, the frontals of *Brachylophosaurus* provide a wide embayment and extensive sutural contact for the nasals (Prieto-Marquez 2005; Evans et al. 2007). The posterodorsal process of the frontal in *Saurolophus* is reminiscent of the dorsal promontorium in *Charonosaurus* and *Parasaurolophus* (Godefroit et al 2001; Evans et al. 2007; Bell 2011). In *Charonosaurus* and *Parasaurolophus*, the underside of the crest is braced by elongate processes of the prefrontals and frontals; those from the prefrontals are longer than the frontal processes (Sullivan and Williamson 1999: fig. 17). As in *Parasaurolophus* (Evans et al. 2007), development of the “dorsal promontorium” in *Saurolophus* is ontogenetically variable. In ZPAL MgD-1/159, the posterodorsal processes of the frontal and prefrontal are short stubs, although the crest

is already well developed at this early stage. An equivalent-sized *Parasaurolophus* braincase described by Evans et al. (2007) has a similar degree of development of the dorsal promontorium. As adults, the posterodorsal processes in *Saurolophus* extend up to half the length of the crest; longer (both relatively and absolutely) than the analogous region in *Parasaurolophus*.

*Saurolophus* is the only dinosaur genus currently recognized from penecontemporaneous beds of both Asia and North America. Despite the fact that there are well-preserved specimens of both species, they have not been described or compared in detail, generating confusion about their cranial anatomy and the validity of the Mongolian taxon (Norman and Sues 2000). Bell (2011) redescribed *S. osborni*; however, the descriptions of *S. angustirostris* provided by Rozhdestvensky (1952, 1957) and Maryńska and Osmólska (1981) were insufficient to permit a comprehensive comparison. The supplementary description and phylogenetic results presented here confirm the close relationship of *S. angustirostris* and *S. osborni*. Although it may be prudent to consider these taxa as separate genera given the considerable geographical separation, a sister group relationship does not require the renaming of either taxon, and the genus name, *Saurolophus* is retained. In addition, it is the author’s opinion that the seven cranial differences listed here do not constitute a difference significant enough to justify distinction at the generic level.

Maryńska and Osmólska (1981) described six cranial characters, which supposedly differentiate the species of *Saurolophus*. However, several of these differences are likely a consequence of comparing juvenile *S. angustirostris* to adult

material of *S. osborni*; specifically, that *S. angustirostris* possesses a relatively shorter lacrimal and external naris, and a relatively longer maxilla. When adult specimens are compared, the proportions of these structures are identical in all cases. This study corroborates two other differences suggested by Maryańska and Osmólska (1981): *S. angustirostris* possesses a more strongly bowed quadrate, and there is a spur on the anterior process of the jugal that separates the lacrimal and maxilla. Although quadrate curvature is difficult to quantify, it is accepted that hadrosaurines typically possess straight quadrates compared to lambeosaurines, which are curved (Horner et al. 2004). Although *S. osborni* conforms to the usual hadrosaurine condition, the quadrate in *S. angustirostris* is bowed as in Lambeosaurinae. The elongate spur on the anterior process of the jugal of *S. angustirostris* is well developed on even the smallest specimen giving the ventral margin of the anterior process a sigmoidal outline. In *S. osborni* this spur is smaller and the ventral margin of the anterior process is convex. Moreover, these differences are maintained across all observed specimens and ontogenetic stages, and therefore are unrelated to preservation or individual variation (contra Norman and Sues 2000). A list of ontogenetic changes identified for *S. angustirostris* in this study are shown in Fig. 12.

Maryańska and Osmólska (1979, 1981) referred to ridges (longitudinal bony septa) on the dorsal surfaces of the nasals in the region of the crest. These were not described for *S. osborni* (Brown 1912), and Maryańska and Osmólska (1981) tentatively regarded this as a specific difference. Although the distal end of the crest is not preserved in *S. osborni*, Bell (2011) did note a series of grooves and ridges on the preserved anterior surface of AMNH 5220, which likely correspond to the ridges described by Maryańska and Osmólska (1981). Longitudinal bony septa, therefore, probably do not distinguish between species of *Saurolophus*.

## Palaeobiogeography

As discussed by Bolotsky and Godefroit (2004), the palaeobiogeography of *Saurolophus* is complex. Fragmentary and scarce hadrosaurine remains from the Amur Region, Russia, have been referred to an apparently closely related form, *Kerberosaurus manakini* (see Bolotsky and Godefroit 2004). *K. manakini* differs from *S. angustirostris* in having a straight quadrate in lateral view; a circumnarial fossa limited posterodorsally by a ridge on the nasal around the naris; a mediolaterally compressed frontal that lacks a posterodorsal process; and a crescent-shaped prefrontal lacking a posterodorsal process. Bolotsky and Godefroit (2004) identified *Kerberosaurus* as “middle” to late Maastrichtian and placed it as the sister taxon to *Saurolophus* and *Prosaurolophus* on account of the frontal being excluded from the orbital rim (Character 5). Results of the phylogenetic analysis presented here place these three taxa in a polytomy, although the apparent absence of a crest in *Kerberosaurus* does indicate a primitive state relative to both *Prosaurolophus* and *Saurolophus*.

The geologically oldest of these three taxa, *Prosaurolophus*, is from the late Campanian of Alberta and Montana. *Saurolophus osborni* is known only from the lower Maastrichtian beds of the Horseshoe Canyon Formation, Alberta (Eberth and Deino 2005; Bell 2011). The Nemegt Formation has not been tightly constrained biostratigraphically, and radiometrically-datable beds are absent. The Nemegt Formation is considered Maastrichtian based on superposition and imprecise biostratigraphy (Jerzykiewicz and Russell 1991; Jerzykiewicz 2000; Shuvalov 2000), but more specific chronostratigraphy is unavailable.

The Beringian land bridge between North America and Asia, which opened during the Aptian–Albian, provided a major dispersal route for terrestrial vertebrates throughout the Late Cretaceous (Russell 1993). The predominant dispersal direction was from west to east, with many Late Cretaceous dinosaur groups—including Neoceratopsia (You and Dodson 2003), Ankylosauridae (Vickaryous et al. 2004), Hadrosauridae (Godefroit et al. 2008), Tyrannosauridae (Serenó et al. 2009), and Troodontidae (Russell and Dong 1993)—supposedly originating in Asia. At higher taxonomic levels, however, dispersal patterns become more complex. Within the Hadrosaurinae, evolution of the clade containing *Kerberosaurus*, *Prosaurolophus*, and *Saurolophus* underwent at least two major dispersal events between Asia and North America. Following the phylogenetic hypothesis of Bolotsky and Godefroit (2004), ancestors of *Kerberosaurus* must have crossed into Asia at or prior to the early late Campanian. Assuming a direct relationship between *Prosaurolophus* and *Saurolophus osborni*, a second dispersal must have taken place at or prior to the earliest Maastrichtian, leading to the evolution of *S. angustirostris*. Alternatively, but less parsimoniously, the most recent common ancestor of *Prosaurolophus* and *Saurolophus* dispersed to Asia at or prior to the early late Campanian and a third dispersal from west to east occurred before the end of the Campanian.

The evolutionary and biogeographic relationship between *S. angustirostris* and *S. osborni* remains unresolved. Therefore, it is unclear which of the two species is more primitive and from which direction the final dispersal took place. Regardless, it is reasonable to suppose that related forms should be present in penecontemporaneous beds in those intervening regions (particularly Alaska, and far eastern Russia and China) that will help elucidate the evolutionary sequence between species of *Saurolophus*.

## Acknowledgements

This paper is dedicated to the memory of late Professor Halszka Osmólska (1930–2008). David Evans, Kevin Seymour (both Royal Ontario Museum, Toronto, Canada), Kieran Shepherd, Mike Feuerstack (both Canadian Museum of Nature, Ottawa, Canada), Carl Mehling (American Museum of Natural History, New York, USA), Magdalena Borsuk-Białynicka (Institute of Palaeobiology, Academy of Science, Warsaw, Poland), Chinzorig Tsogbaatar, Demchig Badamgarov, Rinchen Barsbold (all Mongolian Palaeontological Centre, Ulan Baatar,

Mongolia), Vladimir Alifanov, and Tatyana Tumanova (both Palaeontological Institute, Academy of Science, Moscow, Russia) are thanked for their hospitality and access to specimens in their care. Yuong-Nam Lee (Korean Institute of Geoscience and Mineral Resources, Hwaseong City, South Korea) and the Korean International Dinosaur project generously supported the author's trip to Mongolia. I am indebted to Ariana Paulina Carabajal (Museo Carmen Funes, Plaza Huincul, Argentina) for discussions on braincase anatomy and to Philip Currie, Mike Burns, Victoria Arbour (all University of Alberta, Edmonton, Canada) for comments on an earlier version of the manuscript. Helpful comments by the Editor Rich Cifelli (University of Oklahoma, Norman, USA), and Terry Gates (Utah Museum of natural History, Salt Lake City, Utah, USA), Robin Cuthbertson (University of Calgary, Calgary, Canada), and an anonymous reviewer improved the final version. The Dinosaur Research Institute is gratefully acknowledged for financial support on several museum trips.

## References

- Ali, F., Zelenitsky, D.K., Therrien, F., and Weishampel, D.B. 2008. Homology of the "ethmoid complex" of tyrannosaurids and its implications for the reconstruction of the olfactory apparatus of non-avian theropods. *Journal of Vertebrate Paleontology* 28: 123–133.
- Bell, P.R. 2011. Redescription of the skull of *Saurolophus osborni* Brown 1912 (Ornithischia: Hadrosauridae). *Cretaceous Research* 32: 30–44.
- Bell, P.R. and Evans, D.C. 2010. Revision of the status of *Saurolophus* from California. *Canadian Journal of Earth Sciences* 47: 1417–1426.
- Bell, P.R., Snively, E., and Shychoski, L. 2009. A comparison of the jaw mechanics in hadrosaurid and ceratopsid dinosaurs using finite element analysis. *Anatomical Record* 292: 1338–1351.
- Bolotsky, Y.L. and Godefroit, P. 2004. A new hadrosaurine dinosaur from the Late Cretaceous of far eastern Russia. *Journal of Vertebrate Paleontology* 24: 351–365.
- Brown, B. 1912. A crested dinosaur from the Edmonton Cretaceous. *Bulletin of the American Museum of Natural History* 31: 131–136.
- Currie, P.J. 2009. Faunal distribution in the Nemegt Formation (Upper Cretaceous), Mongolia. In: Y.-N. Lee (ed.), *Annual Report 2008, Korea-Mongolia International Dinosaur Project*, 143–156. Korean Institute Geology and Mineralogy, Seoul, Korea.
- Cuthbertson, R.S. and Holmes, R.B. 2010. The first complete description of the holotype of *Brachylophosaurus canadensis* Sternberg, 1953 (Dinosauria: Hadrosauridae) with comments on intraspecific variation. *Zoological Journal of the Linnean Society* 159: 373–397.
- Edmund, A.G. 1957. On the special foramina in the jaws of many ornithischian dinosaurs. *Royal Ontario Museum Division of Zoology, Palaeontological Contributions* 48: 1–14.
- Eberth, D.A. and Deino, A. 2005. New  $^{40}\text{Ar}/^{39}\text{Ar}$  ages from three bentonites in the Bearpaw, Horseshoe Canyon and Scollard formations (Upper Cretaceous–Paleocene) of southern Alberta, Canada. In: D.R. Braman, F. Therrien, E.B. Koppelhus, and W. Taylor (eds.), *Dinosaur Park Symposium, Short Papers, Abstracts, and Program, Royal Tyrrell Museum, Drumheller, Alberta, September 24–25, 2005*, 23–24. Royal Tyrrell Museum, Alberta.
- Evans, D.C. 2006. Nasal crest homologies and cranial crest function in lambeosaurine dinosaurs. *Paleobiology* 32: 109–125.
- Evans, D.C. 2010. Cranial anatomy and systematics of *Hypacrosaurus altispinus*, and a comparative analysis of skull growth in lambeosaurine hadrosaurids (Dinosauria: Ornithischia). *Zoological Journal of the Linnean Society* 159: 396–434.
- Evans, D.C., Reisz, R.R., and Dupuis, K. 2007. A juvenile *Parasaurolophus* (Ornithischia: Hadrosauridae) braincase from Dinosaur Provincial Park, Alberta, with comments on crest ontogeny in the genus. *Journal of Vertebrate Paleontology* 27: 642–650.
- Gates, T.A. and Sampson, S.D. 2007. A new species of *Gryposaurus* (Dinosauria: Hadrosauridae) from the late Campanian Kaiparowits Formation, southern Utah, USA. *Zoological Journal of the Linnean Society* 151: 351–376.
- Godefroit, P., Hai, S., Yu, T., and Lauters, P. 2008. New hadrosaurid dinosaurs from the uppermost Cretaceous of northeastern China. *Acta Palaeontologica Polonica* 53: 47–74.
- Godefroit, P., Zan, S., and Jin, L. 2001. The Maastrichtian (Late Cretaceous) lambeosaurine dinosaur *Charonosaurus jiyinensis* from north-eastern China. *Bulletin de l'Institut royal des Sciences naturelles de Belgique, Sciences de la Terre* 71: 119–168.
- Heaton, M.J. 1972. The palatal structure of some Canadian Hadrosauridae (Reptilia: Ornithischia). *Canadian Journal of Earth Sciences* 9: 185–205.
- Horner, J. 1983. Cranial osteology and morphology of the type specimen of *Maiasaura peeblesorum* (Ornithischia: Hadrosauridae), with discussion of its phylogenetic position. *Journal of Vertebrate Paleontology* 3: 29–38.
- Horner, J. 1992. Cranial morphology of *Prosaurolophus* (Ornithischia: Hadrosauridae) with descriptions of two new hadrosaurid species and an evaluation of hadrosaurid phylogenetic relationships. *Museum of the Rockies Occasional Paper* 2: 1–119.
- Horner, J.R. and Currie, P.J. 1994. Embryonic and neonatal morphology and ontogeny of a new species of *Hypacrosaurus* (Ornithischia, Lambeosauridae) from Alberta and Montana. In: K.L. Carpenter, K.F. Hirsch, and J.R. Horner (eds.) *Dinosaur Eggs and Babies*, 312–336. Cambridge University Press, Cambridge.
- Horner, J.R., Ricqles, A. de, and Padian, K. 2000. Long bone histology of the hadrosaurid dinosaur *Maiasaura peeblesorum*: growth dynamics and physiology based on an ontogenetic series of skeletal elements. *Journal of Vertebrate Paleontology* 20: 115–129.
- Horner, J.R., Weishampel, D.B., and Forster, C.A. 2004. Hadrosauridae. In: D.B. Weishampel, P. Dodson, and H. Osmólska (eds.), *The Dinosauria, Second Edition*, 438–463. University of California Press, Berkeley.
- Jerzykiewicz, T. 2000. Lithostratigraphy and sedimentary settings of the Cretaceous dinosaur beds of Mongolia. In: M.J. Benton, M.A. Shishkin, D.M. Unwin, and E.N. Kurochkin (eds.), *The Age of Dinosaurs in Russia and Mongolia*, 279–296. Cambridge University Press, Cambridge.
- Jerzykiewicz, T. and Russell, D.A. 1991. Late Mesozoic stratigraphy and vertebrates of the Gobi Basin. *Cretaceous Research* 12: 345–377.
- Lambe, L. 1920. The hadrosaur *Edmontosaurus*. *Geological Survey of Canada, Memoir* 120:1–79.
- Lemmrich, W. 1931. Der Skleralring der Vögel. *Jenaische Zeitschrift für Naturwissenschaft* 65: 514–586.
- Maryańska, T. and Osmólska, H. 1979. Aspects of hadrosaurian cranial anatomy. *Lethaia* 12: 265–273.
- Maryańska, T. and Osmólska, H. 1981. Cranial anatomy of *Saurolophus angustirostris* with comments on the Asian Hadrosauridae (Dinosauria). *Palaeontologia Polonica* 42: 5–24.
- Maryańska, T. and Osmólska, H. 1984. Post-cranial anatomy of *Saurolophus angustirostris* with comments on other hadrosaurs. *Palaeontologia Polonica* 46: 119–141.
- McBratney-Owen, B., Iseki, S., Bamforth, S.D., Olsen, B.R., and Mossiss-Kay, G.M. 2008. Development and tissue origins of the mammalian cranial base. *Developmental Biology* 322: 121–132.
- Morris, W.J. 1973. A review of Pacific coast hadrosaurs. *Journal of Paleontology* 47: 551–561.
- Norman, D. and Sues, H.-D. 2000. Ornithopods from Kazakhstan, Mongolia and Siberia. In: M.J. Benton, M.A. Shishkin, D.M. Unwin, and E.N. Kurochkin (eds.), *The Age of Dinosaurs in Russia and Mongolia*, 462–479. Cambridge University Press, Cambridge.
- Ostrom, J.H. 1961. Cranial morphology of the hadrosaurian dinosaurs of North America. *Bulletin of the American Museum of Natural History* 122: 33–186.
- Prieto-Marquez, A. 2005. New information on the cranium of *Brachylophosaurus canadensis* (Dinosauria, Hadrosauridae), with a revision of its phylogenetic position. *Journal of Vertebrate Paleontology* 25: 144–156.
- Prieto-Marquez, A. 2010. Global phylogeny of Hadrosauridae (Dinosauria:

- Ornithopoda) using parsimony and Bayesian methods. *Zoological Journal of the Linnean Society* 159 (2): 435–502.
- Riabinin, A.N. 1930. Towards a problem of the fauna and age of dinosaur beds on the Amur River [in Russian with English summary]. *Russkoe Paleontologičeskoe Obščestvo, Monografy* 11: 41–51.
- Rozhdestvensky, A.K. 1952. A new representative of duckbilled dinosaurs from the Upper Cretaceous deposits of Mongolia [in Russian]. *Doklady Akademii SSSR* 86: 405–408.
- Rozhdestvensky, A.K. 1957. The duck-billed dinosaur *Saurolophus* from the Upper Cretaceous of Mongolia [in Russian]. *Vertebrate Palaeontologia* 1: 129–149.
- Rozhdestvensky, A.K. 1965. Growth changes in Asian dinosaurs and some problems of their taxonomy [in Russian]. *Paleontologičeskij žurnal* 3: 95–109.
- Russell, D.A. 1993. The role of central Asia in dinosaurian biogeography. *Canadian Journal of Earth Sciences* 30: 2002–2012.
- Russell, D.A. and Chamney, T.P. 1967. Notes on the biostratigraphy of dinosaurian and microfossil faunas in the Edmonton Formation (Cretaceous), Alberta. *National Museum of Canada Natural History Papers* 35: 22.
- Russell, D.A. and Dong, Z.-M. 1993. A nearly complete skeleton of a new troodontid dinosaur from the Early Cretaceous of the Ordos Basin, Inner Mongolia, People's Republic of China. *Canadian Journal of Earth Science* 30: 2163–2173.
- Russell, L.S. 1940. The sclerotic ring in the Hadrosauridae. *Royal Ontario Museum Palaeontology Contributions* 3: 1–7.
- Sereno, P.C., Tan, L., Brusatte, S.L., Kriegstein, H. J., Zhao, X., Cloward, K. 2009. Tyrannosaurid skeletal design first evolved at small body size. *Science* 326: 418–422.
- Shuvalov, V.F. 2000. The Cretaceous stratigraphy and palaeobiogeography of Mongolia. In: M.J. Benton, M.A. Shishkin, D.M. Unwin, and E.N. Kurochkin (eds.), *The Age of Dinosaurs in Russia and Mongolia*, 256–278. Cambridge University Press, Cambridge.
- Sullivan, R.M. and Williamson, T.E. 1999. A new skull of *Parasaurolophus* (Dinosauria: Hadrosauridae) from the Kirtland Formation of New Mexico and a revision of the genus. *New Mexico Bulletin of Natural History and Science* 15: 1–52.
- Swofford, D.L. 2002. *Phylogenetic analysis using parsimony (and other methods)*. Version 4.0b10. 40 pp. Sinauer Associates, Sunderland, Massachusetts.
- Vickaryous, M.K., Maryańska, T., and Weishampel, D.B. 2004. Ankylosauria. In: D.B. Weishampel, P. Dodson, and H. Osmólska (eds.), *The Dinosauria, Second Edition*, 363–392. University of California Press, Berkeley.
- Weishampel, D.B. and Horner, J.R. 1990. Hadrosauridae. In: D. Weishampel, P. Dodson, and H. Osmólska (eds.), *The Dinosauria, Second Edition*, 534–561. University of California Press, Berkeley.
- Weishampel, D.B., Norman, D.B., and Grigorescu, D. 1993. *Telmatosaurus transylvanicus* from the Late Cretaceous of Romania: the most basal hadrosaurid dinosaur. *Palaeontology* 36: 361–385.
- Weishampel, D., Barrett, P., Coria, R., Le Loeuff, J., Xu, X., Zhao, X., Sahni, A., Goman, E., and Noto, C. 2004. Dinosaur distribution. In: D. Weishampel, P. Dodson, and H. Osmólska (eds.), *The Dinosauria, Second Edition*, 517–606. University of California Press, Berkeley.
- You, H.-L. and Dodson, P. 2003. Redescription of neoceratopsian dinosaur *Archaeoceratops* and early evolution of Neoceratopsia. *Acta Palaeontologica Polonica* 48: 261–272.
- Young, C.C. 1958. The dinosaurian remains of Laiyang, Shantung. *Palaeontologia Sinica* 16: 53–138.